VER
Vascular & Endovascular Review

The possible effect of Adipose-derived Stromal Vascular Fraction Cells on Hair Growth in rat model of Androgenic Alopecia: Histological and Immunohistochemical Study

Medhat Atta Salah[1,3], Abdel Hamid Sayed Abo Bakr[1,3], Mohamed Ahmed Desouky[1,3], Mary Malak Reyad[1,3,] Manar Fouli Gaber Ibrahim[2,4,5]

[1]Department of Anatomy and Embryology, Faculty of Medicine, Minia University, Minia, Egypt;
[2]Department of Histology and Cell Biology, Faculty of Medicine, Minia University, Minia, Egypt;
[3]Department of Anatomy and Embryology, Faculty of Medicine, Minia National University, Minia, Egypt;
[4]Department of Histology and Cell Biology, Faculty of Medicine, Minia National University, Minia, Egypt;
[5]Faculty of Physical Therapy, Lotus University, Minia, Egypt. manar.fouli@lum.edu.eg

ABSTRACT

Background: Androgenic alopecia (AGA) is a common progressive hair loss condition that is mostly mediated by dihydrotestosterone (DHT). In this context, Stromal vascular fraction (SVF) cells are capable of restoration hair follicle structure and promoting hair growth as they contain regenerative and immunomodulatory cells.
Aim: the study investigated the therapeutic effect of SVF using a rat model of androgenic alopecia.
Materials and Methods: 60 male albino rats were separated into 4 groups: group I (control; subdivided into Ia negative control and Ib positive control injected with SVF), group II (testosterone-induced alopecia), group III (SVF-treated), and group IV (recovery). Alopecia was induced by daily subcutaneous testosterone injection for three weeks. Group III subsequently received a single injection of 2×10^6 SVF cells. Skin and serum samples were obtained for histological, immunohistochemical, and biochemical analysis.
Results: Alopecia-group (group II) resulted in follicular miniaturization, epidermal thinning, and disruption of collagen fibers in the dermis. Immunohistochemical staining demonstrated weak Ki-67 and strong activated caspase-3 expression, while biochemical analysis revealed increased serum level of testosterone, malondialdehyde (MDA), and DKK1 with decreased glutathione (GSH) and WNT3l levels. SVF-treated rats (group III) displayed marked improvement of epidermal thickness, follicular architecture and collagen organization. SVF also attenuated caspase-3 overexpression, increased Ki-67 proliferative activity, it resulted in decreased oxidative stress along with significant correction of androgen- and WNT-related biochemical alterations, bringing them near-control levels.
Conclusion: In androgen-induced alopecia, adipose-derived SVF demonstrated strong regenerative, anti-apoptotic, and antioxidant properties, underscoring its potential as a novel therapeutic approach for hair follicle regeneration.

KEYWORDS: Androgenic Alopecia, Stromal Vascular Fraction, Hair Follicle Regeneration, Oxidative Stress, Apoptosis.

How to Cite: Medhat Atta Salah, Abdel Hamid Sayed Abo Bakr, Mohamed Ahmed Desouky, Mary Malak Reyad, Manar Fouli Gaber Ibrahim., (2025) The possible effect of Adipose-derived Stromal Vascular Fraction Cells on Hair Growth in rat model of Androgenic Alopecia: Histological and Immunohistochemical Study, Vascular and Endovascular Review, Vol.8, No.9s, 383--402.

INTRODUCTION

Androgenic alopecia (AGA) is the predominant type of progressive hair loss, affecting both genders. It may begin as early as the second decade of life, and its prevalence rises with age.

Androgens are the main cause in those who are genetically susceptible. Histologically, AGA is defined by progressive reduction in hair follicular size, whereby thick terminal hairs are replaced by finer vellus hairs [1].

Hair follicles go through a dynamic cycle process under normal physiological conditions, which consists of a growth phase (anagen), a regression phase (catagen), a resting phase (telogen), and a shedding phase (exogen). In AGA, the anagen phase is shortened whereas the telogen phase is extended so the balance is disturbed resulting in a decreased anagen-to-telogen hair ratio [2].

The pathophysiology of AGA involves a complex interaction of genetic, hormonal, and environmental variables. In predisposed individuals, testosterone is converted to dihydrotestosterone (DHT) by 5α-reductase type II in dermal papilla cells, which enhances androgen receptor activity and induces inhibitory mediators such as Dickkopf-1 (DKK-1), while simultaneously suppressing growth factors critical for anagen maintenance [3]. These alterations reduce the duration of the anagen phase, extend the telogen phase, and promote the transformation of thick hairs into fine hairs.

Hair cycle impairment is exacerbated by genetic alterations in the androgen receptor (AR) gene and chromosome 20p11, which further disrupt the signaling of Wnt/β-catenin pathway which plays a crucial role involved in regulation of hair cycling, especially throughout the shift from telogen to anagen [4]. DHT inhibits this pathway through the production of DKK-1, an endogenous Wnt antagonist, this disruption prevents follicle regeneration, resulting in progressive miniaturization and inability to reenter the

growth phase [4]. Treatment of AGA aims to avoid and reverse the process of miniaturization. A variety of therapeutic modalities exist, including medication, surgical procedures, and novel regenerative approaches [5].

Regenerative treatments have recently garnered interest owing to their efficacy in hair restoration by targeting the underlying disease-related pathways [6]. These encompass platelet-rich plasma injections, micro-needling, and cell-based therapies, including adipose-derived stromal vascular fraction (SVF) and stem cell applications, which seek to improve follicular regeneration via growth factors and modulation of the hair follicle microenvironment [7].

SVF is a cellular population extracted from subcutaneous fat via enzymatic or mechanical digestion. SVF comprises mesenchymal stem cells, endothelial progenitors, pericytes, and immune cells, all of which enhance its healing capacity, rendering it a viable treatment alternative for androgenetic alopecia [6].

This study examined the impact of adipose-derived stromal vascular fraction (SVF) cells on hair growth in a rat model of androgenetic alopecia, employing histological and immunohistochemical analysis.

MATERIALS AND METHODS

Animals and Ethical Approval:

This research constitutes an experimental investigation. The study was done in the Department of Anatomy and Embryology, Faculty of Medicine, Minia University, Egypt. The study used 60 adult male albino rats aged 10-12 weeks, with weights ranging from 200 to 220 grams. Furthermore, ten male albino rats aged 4-6 weeks, with a weight range of 70-80 grams, were utilized as a source of adipose-derived stromal vascular fraction (SVF) cells. All experimental protocols were carried out following the local rules established by the ethics council of the Faculty of Medicine, Minia University (Approval number. 932/10/2023).

Chemicals and Reagents:

Testosterone was obtained in the form of Testonon ® 250 mg/mL (testosterone enanthate; Cat. No. 231277, Nile Company for Pharmaceuticals and Chemical Industries, Egypt).
Collagenase type I (Cat. No.C0130, Sigma-Aldrich, Egypt).
Dulbecco's Modified Eagle Medium (DMEM) (Cat.No. D6546, Sigma-Aldrich, Egypt).
Phosphate Buffered Saline (PBS) (Cat. No. P3813, Sigma-Aldrich, Egypt) .
Antibodies: Anti-activated Caspase-3 (apoptotic, CAT#ab32351, Abcam, Egypt,) and anti-Ki-67 (proliferation, CAT#ab15580, Abcam, Egypt, CAT#ab15580).

Enzyme-linked immunosorbent assay (ELISA) kits for estimating the following:
Serum Testosterone (Catalogue No.CSB-E05100r, Bio-diagnostic, Egypt).
Serum Malondialdehyde (MDA) (Catalogue No.MD 25 29, Bio-diagnostic, Egypt).
Serum Reduced Glutathione (GSH) (Catalogue No.GR 25 11, Bio-diagnostic, Egypt).
Serum Wingless-related integration site 3(WNT3) (Catalogue No. RTDL01115, Bio-diagnostic, Egypt).
Tissue Dickkopf-related protein 1(DKK1) (Catalogue No.TR 118, Bio-diagnostic, Egypt).

Induction of Androgenic Alopecia:

Testosterone (0.1 ml) was injected subcutaneously into the shaved dorsal area once daily for 21 consecutive days to induce androgenic alopecia.

Preparation of stromal vascular fraction cells (SVFCs):

1-Procurement of Adipose Tissue: from the abdominal fat of 10 healthy donor rats. Approximately 2–3 grams of adipose tissue were taken and promptly immersed in a septic phosphate-buffered saline (PBS) with 1% penicillin-streptomycin to avert microbial contamination [8].

2-Processing the Adipose Tissue: Under a laminar flow hood, the tissue was placed in a 35 mm tissue culture dish containing HBSS (Hank's Balanced Salt Solution) for thorough cleaning using sterile forceps. The adipose tissue was subsequently cut into minute fragments with sterile scissors and transferred into sterile 50 ml centrifuge tubes. Subsequently, 5 ml of collagenase solution per gram of adipose tissue was introduced into each centrifuge tube. The centrifuge tubes were sealed, disinfected with 70% ethanol, and subsequently covered in parafilm before to being placed in the incubator. Each tube was agitated at 100 rpm for 60 minutes until the tissue appeared smooth.

3-Isolation of the Stromal Vascular Fraction (SVFCs):
Enzymatic Digestion:
The tissue was finely chopped into small fragments (about 1–2 mm^3) using sterile scissors and subsequently digested in 0.1% collagenase type I (Sigma-Aldrich) dissolved in PBS. The digestion occurred at 37°C in a shaking water bath or orbital shaker at 150–200 rpm for 30–45 minutes. Gentle pipetting was performed every 10 minutes to guarantee complete enzymatic interaction [8].

Separation and Washing:

The processed mixture was filtered through a 100 µm sterile nylon mesh to exclude undigested particles. The filtrate underwent centrifugation at 1500 rpm for 10 minutes at ambient temperature, resulting in the deposition of the stromal vascular pellet. The supernatant, which included mature adipocytes and enzymatic residues, was discarded. The pellet underwent two washes in serum-free DMEM, utilizing moderate centrifugation (1000 rpm for 5 minutes) between washes to eliminate remaining enzymes. The stromal vascular fraction cells were seen as dark red cells sedimented at the bottom. The oil at the surface and the primary adipocytes, which manifested as a yellow layer of suspended cells, were meticulously aspirated. A minimal quantity of brown collagenase solution remained, ensuring the pelleted stromal vascular fraction cells were undisturbed.

4-Detection of SVFCs viability and quantity:
The cell pellet was reconstituted in 1 ml of DMEM enriched with 1% fetal bovine serum (FBS). Viable nucleated cells were enumerated with a hemocytometer following trypan blue staining. A cell viability threshold of 85% was deemed acceptable. A suspension of 2×10^6 viable SVF cells in 200–300 µl of DMEM was prepared for injection. The final SVF preparation was delivered subcutaneously in the dorsal region of Group III animals at the previously shaved and testosterone-injected site. SVF injections were conducted within 2 hours of isolation to guarantee cell viability and biological activity [9]

Experimental design:
An area of 1cm x1cm on the dorsal region of the rats was delineated. Sixty adult male albino rats were utilized in this experiment, allocated into four groups (n = 15 each group).
Group I (Control): was separated into two subgrups:
group Ia (Negative control): received no treatment
group Ib (Positive control): was given a single a single subcutaneous injection of 2×10^6 SVF cells into the dorsal skin area [10].
Group II (Alopecia-group): was given a single subcutaneous injection of 0.1 ml testosterone into the dorsal skin daily for 3weeks to induce androgenic alopecia [11].
Group III (SVF-treated): received subcutaneous injection of 0.1 ml testosterone into the dorsal skin daily for 3weeks followed by a single subcutaneous injection of 2×10^6 SVF cells into the same area [10]
Group IV (Recovery): received subcutaneous injection of 0.1 ml testosterone into the dorsal skin daily for 3 weeks, followed by no treatment for remainder of the duration [12].

The experiment was concluded by the sacrifice of the animals in Groups I and II at the end of the third week, while the animals in Groups III and IV were scarified at the end of the sixth week. The dorsal skin at the injection location was removed. Blood specimens and skin tissues were taken. Blood samples were obtained by heart puncture using a needle attached to a 5 ml syringe for biochemical analysis. The skin tissues were excised and irrigated with normal saline. Tissues were fixed in a 10% neutral formalin for 24 twenty-four hours, subsequently rinsed with running water, and prepared as paraffin slices for histological and immunohistochemical analysis.

Biochemical analysis:
Blood was collected and let to coagulate at ambient temperature. Serum was isolated using centrifugation at 3000 rpm for 15 minutes and thereafter were stored at −20 °C prior to analysis. Skin tissues were prepared as a tissue suspension in PBS and preserved at −80 °C. The following biochemical parameters were assessed according to the manufacturer's instructions:
a- Serum Testosterone: Measured using a rat-specific ELISA kit (Cat. No. CSB-E05100r; Bio-diagnostic, Egypt).
b- Serum Malondialdehyde (MDA): Determined spectrophotometrically as a marker of lipid peroxidation (Cat. No. MD 25 29; Bio-diagnostic, Egypt).
c- Serum Reduced Glutathione (GSH): Quantified colorimetrically using a commercial kit (Cat. No. GR 25 11; Bio-diagnostic, Egypt).
d- Serum WNT3 Protein: Measured by rat-specific ELISA (Cat. No. RTDL01115; Bio-diagnostic, Egypt).
e- Tissue DKK1: Evaluated by quantitative real-time PCR (qRT-PCR) in skin homogenates (Cat. No. TR 118; Bio-diagnostic, Egypt). Additionally, DKK1 protein levels in tissue homogenates were quantified using ELISA, following kit protocols. All biochemical assays were conducted at the Pharmacology Department, Faculty of Medicine, Minia University.
I. Histological Study
All specimens were collected, preserved in 10% neutral-buffered formalin followed by tissue dehydration in successive concentrations of ethyl alcohol, cleaned in xylene, impregnated with soft paraffin, followed by hard paraffin, and sectioned to a thickness of 5 µm. Sections were stained with Hematoxylin and Eosin to assess the overall histology of the skin and hair follicle, and with Mallory's trichrome to visualize collagen fibers [13]:

IMMUNOHISTOCHEMICAL STUDY

The immunohistochemical staining was conducted according to the manufacturer's instructions. In summary, skin slices were subjected to deparaffinization and rehydration. Endogenous peroxidase activity was inhibited by the application of 0.01% hydrogen peroxide for 10 to 15 minutes at 37°C. Sections underwent antigen retrieval by being incubated in EDTA solution and subjected to microwave treatment for 20 minutes. Subsequently, slices were treated with primary antibodies at 4°C overnight. The principal antibodies employed were anti-activated caspase-3 antibody (apoptotic, CAT#ab32351; Abcam, Egypt) and anti-Ki-67 antibody (proliferation, CAT#ab15580; Abcam, Egypt). Subsequently, slices were submerged in a secondary antibody for 30 minutes, followed by washing and a 20-minute incubation with the HRP (horseradish peroxidase) Envision kit (DAKO). Sections were rinsed and treated with diaminobenzidine (DAB) for 15 minutes. Hematoxylin was employed for counterstaining the nuclei. Negative control sections were acquired by processing sections using the same technique, but with the exclusion of

the main antibody. The positive control for activated caspase-3 utilized rat thymus tissue, whereas the positive control for Ki-67 employed rat tonsil tissue, to confirm the specificity and reproducibility of the staining protocol. Immunoreactivity was seen as dark brown cytoplasmic staining. Ki-67 expression was localized to the nucleus, but activated caspase-3 expression was seen in both nuclear and cytoplasmic compartments [14]:

Image capture:
Photomicrographs of H&E, Mallory's trichrome, and immunostained sections were obtained using a BX51 light microscope (Olympus, Japan) with a high-resolution digital camera, connected to LC micro application software at the Histology and Cell Biology Department, Faculty of Medicine, Minia University.

IV) Morphometric Study
Morphometric analysis was done on histological and immunohistochemical sections to evaluate the following parameters:
Epidermal thickness, area percentage of Masson's trichrome stained sections and activated Caspase-3 immunopositivity were measured using Image J software (http://rsbweb.nih.gov/ij/; NIH, Bethesda)
The number of hair follicles, Ki-67 positive nuclei and number of activated Caspase-3 positive nuclei was quantified. All parameters were evaluated in five consecutive non-overlapping fields from each rat in each group at a magnification of ×400.The histologist was blind for the different experimental groups.

V) Statistical Analysis
Quantitative data were analyzed using Graph Pad Prism (version 7.01 for Windows, Graph Pad Software, San Diego, California, U.S.A., www.graphpad.com). The mean and standard error of the mean (SEM) were computed for the parameters of each group. Values were presented as Mean ± SEM. Significant differences between each pair of groups were assessed using the student t-test, while one-way ANOVA followed by the Tukey-Kramer post hoc test was employed for multiple comparisons. P-values less than 0.05 are deemed statistically significant.

RESULTS

1. Biochemical Results:

1.1. serum testosterone level:
The results showed that there was a significant increase ($P<0.05$) in the serum level of testosterone in the Alopecia and Recovery groups compared to the control group. In the SVF-treated group, the serum testosterone level showed a significant increase ($P< 0.05$) compared to the control group However, there was a significant decrease ($P< 0.05$) when compared to the Alopecia- group. Additionally, the SVF- group also exhibited a significant decrease ($P< 0.05$) compared to the Recovery group. While there was insignificant difference ($P > 0.05$) in level of testosterone in recovery group compared to alopecia- group (Figure 1a).

1.2. serum level of Malondialdehyde (MDA):
The serum level of MDA showed a significant increase ($P< 0.05$) in Alopecia and Recovery groups compared to the control group. In the SVF-treated group, there was a significant increase ($P< 0.05$) compared to the control group and a highly significant decrease ($P< 0.05$) compared to the Alopecia group. Moreover, the MDA level in the SVF group was also significantly lower than that in the Recovery group ($P< 0.05$). While there was insignificant difference ($P > 0.05$) in level of MDA in recovery group compared to alopecia group (Figure1b).

1.3. serum level of Reduced Glutathione (GSH):
The serum level of GSH results was significantly decrease in in Alopecia- and Recovery groups compared to the control group. SVF-treated group showed a significant increase in the serum level of GSH compared to both the Alopecia group ($P< 0.05$) and the Recovery group ($P< 0.05$). While there was insignificant difference ($P > 0.05$) in level of GSH in recovery group if compared to alopecia group (Figure 1c)

1.4. serum level of WNT3:
The results showed that there was a significant decrease in the level of WNT3 protein in the Alopecia and recovery groups compared to the control group (p value<0.05). SVF-treated group showed a significant increase (p value<0.05) compared to both the Alopecia- and Recovery groups. While there was insignificant difference ($P > 0.05$) in level of WNT3 in recovery group if compared to alopecia group (Figure 1d)

1.5. Tissue level of Dickkopf-1 (DKK1):
The results revealed that there was a significant increase (p value<0.05) in DKK1 levels in the alopecia- group compared to the control group. The SVF-treated group showed a significant decrease (p value<0.05) compared to the alopecia group. While the recovery group demonstrated no significant difference ($P >0.05$) compared to the alopecia group, but showed a significant increase (p value<0.05) in DKK1 levels compared to both the control and SVF-treated groups (Figure 1e).

2. Histological Results:

A. Hematoxylin and Eosin (H&E) stains results:
Analysis of the skin samples from Group I:
The examination revealed typical architecture composed of three distinct layers: the epidermis, dermis, and hypodermis. The dermis showed prominent dermal papillae interdigitating with the epidermis and contained many hair follicles surrounded by

sebaceous glands of normal histology (Figure 2a). The epidermis was composed of well-organized successive layers, including the stratum basale formed of a single row of columnar cells with basophilic cytoplasm and basal oval vesicular nuclei ,the stratum spinosum consisted of polygonal cells with basophilic cytoplasm and central rounded vesicular nuclei, the stratum granulosum composed of one to two layers of flattened cells with basophilic granules, and the stratum corneum which composed of flattened, a nucleated, keratinized cells (Figure 2b).

The dermis displayed intact papillary and reticular layers with a well-preserved dermo-epidermal junction (Figure 2b). Hair shaft was composed of medulla, cortex, and cuticle, which were surrounded by the inner root sheath, outer root sheath, and connective tissue sheath (Figure 2c). The hair bulb consisted of dermal papilla cells which are fibroblast-like and adjacent polygonal matrix cells (Figure 2d). Sebaceous glands presented as acinar structures originating from the outer root sheath, consisting of vacuolated cuboidal cells lined by flattened basal cells (Figure 2e). The telogen hair follicles showed the hair bulb was replaced by a dermal papilla containing secondary hair germ cells (Figure 2f).

Examination of skin sections of the alopecia-group (Group II) showed a marked decrease in epidermal thickness with loss of the stratum corneum and decrease in the number of hair follicles. The epidermis showed marked alterations, including distorted cells, cytoplasmic vacuolation, and deeply stained eccentric nuclei eccentric nuclei Hair root layers exhibited disruption and degeneration with separation of follicular layers and presence of degenerated follicles. The hair bulbs showed vacuolation of dermal papilla and matrix cells Sebaceous glands appeared lobulated. Catagen and telogen follicles predominated over anagen follicles; catagen follicles were distinguished by epithelial strands linking dermal papillae to club hairs. The blood vessels in the dermis were congested, (Figures 3,4,5).

Histological sections of the SVF-treated group (Group III) the examination showed a noticeable increase in the thickness of epidermis and a notable increase in hair follicles count, with restoration of normal skin structure. The epidermis regained its normal stratification and exhibited well-organized layers, including stratum basale, spinosum, granulosum, and corneum. Anagen follicles predominated over telogen follicles and extended deep into the dermis and hypodermis. Sebaceous glands appeared normal, and club hairs were noted, suggesting follicles in late telogen or early anagen stages. Matrix cells forming new hair shafts were also observed (Figure 6)

Skin sections of Recovery group (Group IV) revealed decreased epidermal thickness and reduced hair follicle number. Degeneration of hair follicles was evident, with swelling and vacuolation of dermal papilla and matrix cells. Catagen follicles were distinguished by epithelial strands connecting dermal papillae to club hairs. Sebaceous glands appeared lobulated with acinar morphology (Figure 7).

B. Mallory's Trichrome Stain Results:
Examination of specimens from the control group revealed thin, delicate, and irregularly arranged collagen fibers in the papillary dermis, whereas the reticular dermis showed coarse, wavy, and regularly arranged collagen bundles (Figure 8a, b). While, examination of the alopecia -group showed a marked widening and separation between dermal collagen fibers (Figure 8c–f). The SVF-treated group revealed a restoration of collagen architecture toward the normal, marked by regularly arranged fibers and showed noticeable reduction in collagen fiber widening and separation (Figure 8g, h). However, in the recovery group, collagen fibers remained widened and separated within the dermis (Figure 8i, j).

3. Immunohistochemical Results

3.1. Ki67 Immunoreactivity:
Ki67-stained sections of the control group revealed many cells with positive nuclear expression Primarily confined to the basal cell layer and extending into the prickle cell layer of the epidermis, as well as within hair follicles. (Figure 9a, b). In the alopecia group, Ki67 expression was markedly reduced, with only scattered positively stained nuclei in the stratum basale and within the follicular components (Figure 9c). The SVF-treated group exhibited numerous Ki67-positive nuclei in both the basal and prickle cell layers, along with strong positive nuclear expression within hair follicles (Figure 9d, e). In the recovery group, only a few positively stained nuclei were observed in the stratum basale and within the follicular components (Figure 9f, g).

3.2. Activated Caspase-3 Immunoreactivity:
The examination of the control group displayed faint cytoplasmic expression in epidermal cells, with negative nuclear and cytoplasmic expression in the inner and outer root sheath of hair follicles (Figure 10a, b). While the alopecia-group (II) showed numerous epidermal cells with positive nuclear expression, along with strong nuclear and cytoplasmic positivity in the outer root sheath of hair follicles (Figure 10c, d). Examination of the SVF-treated group (III) revealed faint nuclear positivity in epidermal cells, whereas both the inner and outer root sheath of hair follicles exhibited negative expression (Figure 10e, f). The recovery group (IV) showed many epidermal cells with positive nuclear and cytoplasmic expression, together with positive expression in the outer root sheath of hair follicles (Figure 10g, h).

4. Morphometric study:
A. Epidermal thickness: The epidermal thickness was measured in all groups and the results showed that group II displayed a significant decrease ($P<0.05$) compared to the control group. While SVF-treated group showed a significant increase ($P<0.05$) compared to Alopecia-group. However, there was no significant difference ($P>0.05$) between SVF-treated and the control group.

The recovery group showed a significant decrease (P<0.05) compared to both control and svf-treated group, while there was no significant difference (P>0.05) when compared alopecia-group (Figure 11a)

B. Total number of hair follicles: The total number of hair follicles was significantly decreased in alopecia-group compared to the control group (P<0.05). SVF-treated group showed a significant increase (P<0.05) compared to alopecia-group, with no significant difference (P>0.05) when compared to the control group. Meanwhile, the recovery group displayed a significant decrease (P<0.05) compared to both control and SVF-treated groups, while no significant difference was observed compared to alopecia-group. (Figure 11b)

C. Area percentage of collagen fibers: the results demonstrated that there was a significant decrease (P < 0.05) in the alopecia-group compared to the control group. The SVF-treated group showed a significant increase compared to the alopecia-group (P < 0.05), with no significant difference from the control group (P > 0.05). The recovery group showed a significant decrease compared to both the control and SVF-treated groups (P < 0.05), while showed no significant difference when compared to the alopecia group (P > 0.05). (Figure 11c).

D. Number of Ki-67 positive cells: The alopecia-group showed a significant decrease in positive cells in the stratum basale , inner and outer root sheath, and matrix cells compared to the control group (P<0.05). Svf-treated group showed a significant increase (P<0.05) compared to both control and alopecia-group. While the recovery group displayed a significant decrease (P<0.05) compared to control and SVF-treated groups, and no significant difference (P>0.05) compared to alopecia-group. (Figure 11d)

E. Mean area fraction of activated caspase-3 immunoreactivity: Alopecia-group showed a significant increase in mean area fraction of activated caspase-3 compared to the control group (P<0.05). SVF-treated group revealed a significant decrease (P<0.05) compared to alopecia-group. While the recovery group displayed a significant increase (P<0.05) compared to both control and SVF-treated groups, with no significant difference (P>0.05) was observed when compared to alopecia-group (Figure 11e).

F. Number of activated caspase-3 positive cells: The number of activated caspase-3–positive cells was significantly increased in the alopecia- group compared to the control group (P < 0.05). The SVF-treated group revealed a significant decrease relative to alopecia-group (P < 0.05) and no significant difference compared to the control (P > 0.05). The recovery group showed a significant increase compared to control and svf-treated group (P < 0.05), while no significant difference was observed relative to alopecia-group (P > 0.05). (Figure 11f).

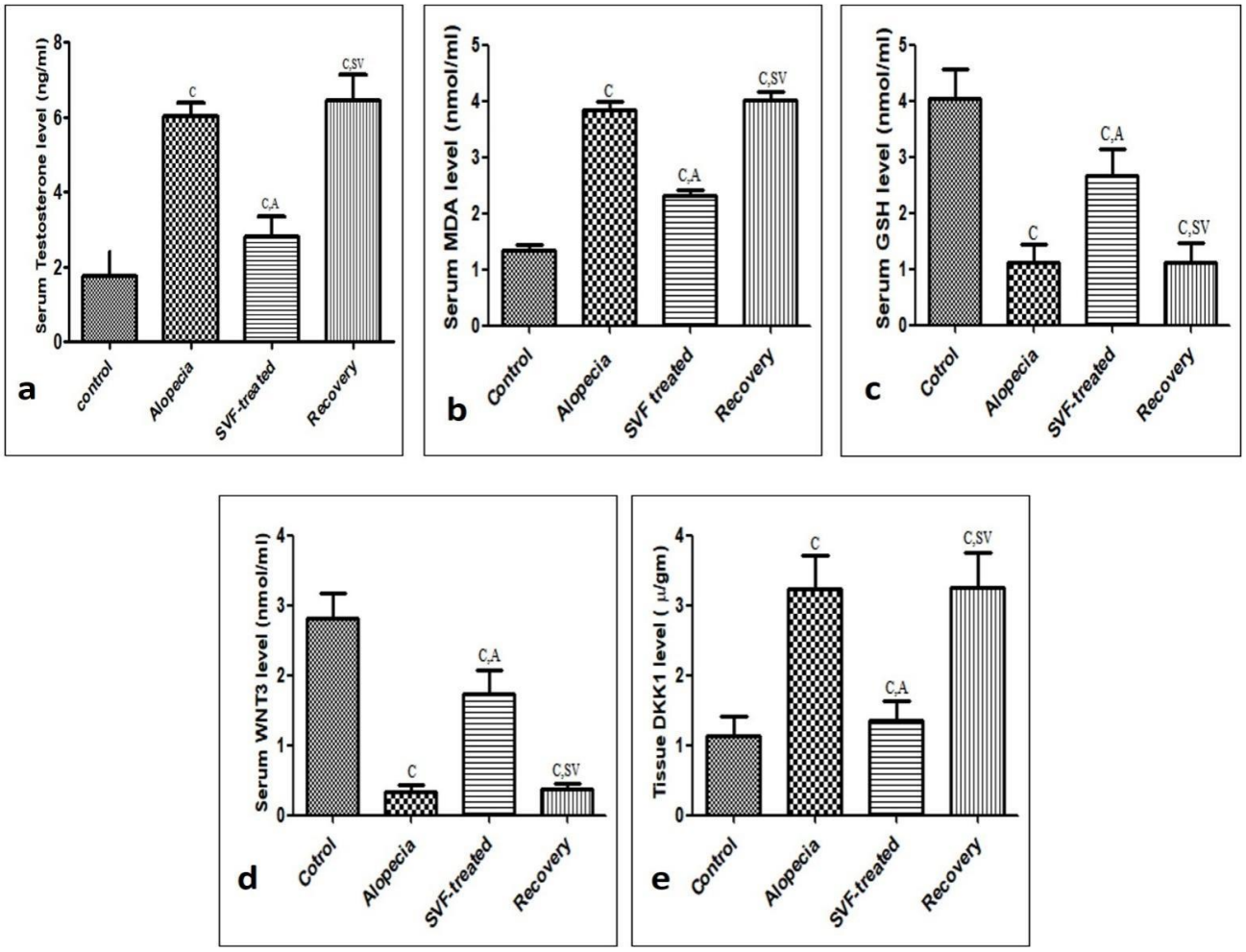

Figure 1. Bar charts showing the biochemical parameters in the experimental groups. (a) mean level of serum testosterone (ng/ml). (b) mean level of serum malondialdehyde (MDA)(nmol/ml). (c) mean level of serum reduced glutathione (GSH) (nmol/ml). (d)

mean level of serum WNT3 (nmol/ml). (e) mean level of tissue Dickkopf-1 (DKK1) (m/gm). Data are expressed as mean ± SD. Significant differences: c versus control group, A versus alopecia group, sv versus SVF-treated group. $p < 0.05$ is significant.

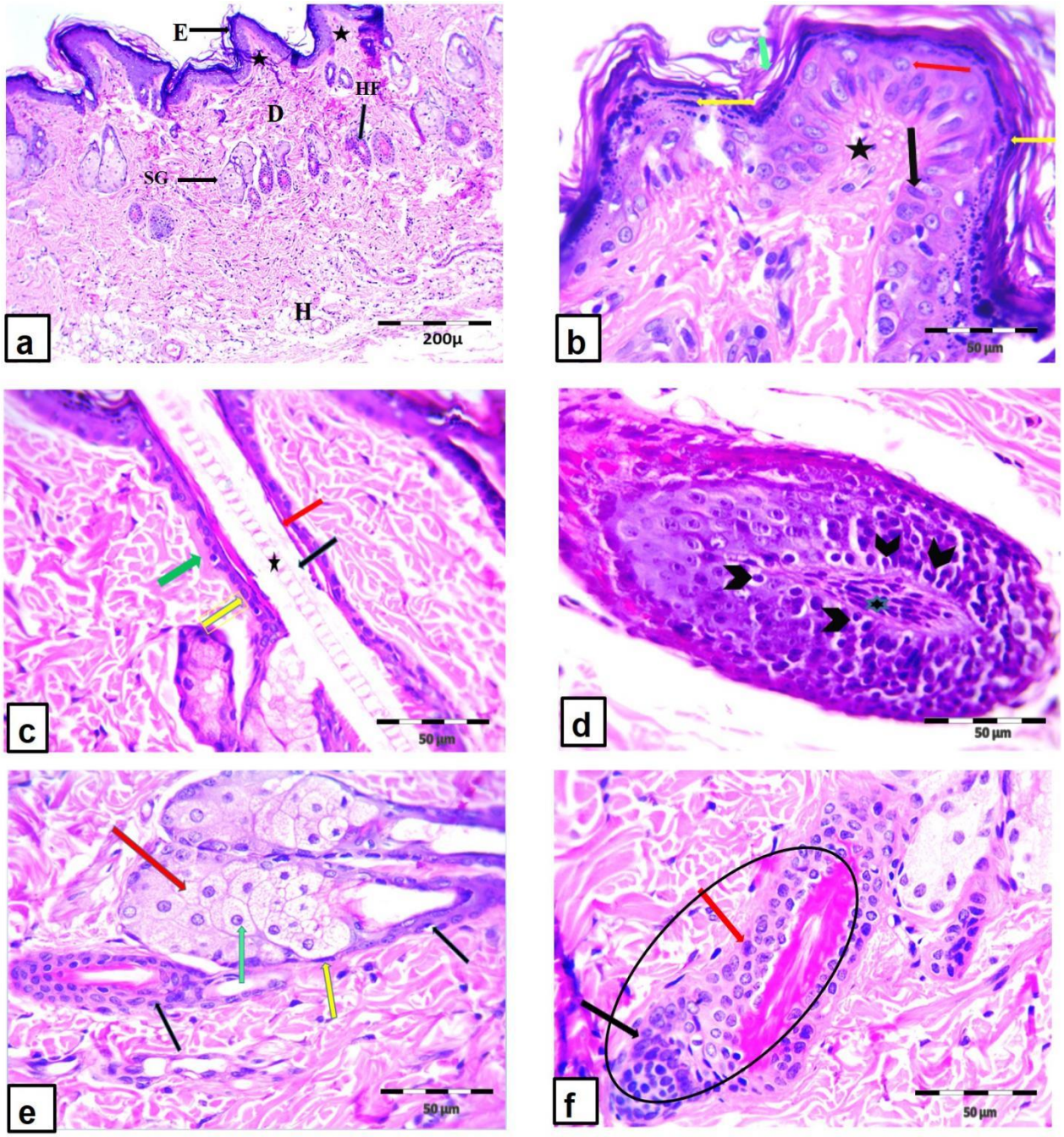

Figure 2: Representative photomicrographs of H&E-stained skin sections of group I (control): (a) Showing the general architecture of the skin; epidermis (E), dermis (D), and hypodermis (H). Dermal papillae (★), The dermis clearly displays hair follicles (HF) and sebaceous glands (SG). (b) illustrating the layers of the epidermis: stratum basale (black arrow), stratum spinosum (red arrow), stratum granulosum (yellow arrows), and stratum corneum (green arrow). Dermal papillae (★) are also visible. (c) Showing a hair root with medulla (★), cortex (black arrow), inner root sheath (red arrow), outer root sheath (yellow arrow), and connective tissue sheath (green arrow). (d) Showing a longitudinal section of an anagen hair bulb. Dermal papilla cells (★) and matrix cells (arrowheads) are evident. (e) Showing dermis containing hair follicles (black arrows) attached to sebaceous glands (red arrow) which composed of several layers of cuboidal vacuolated cells (green arrow) resting on a basal layer of flattened cells (yellow arrow). (f) Illustrating a telogen hair follicle. The telogen germinal unit (circle) formed of dermal papilla (black arrow) and secondary hair germ (red arrow) is observed. (a:H&E ×100; scale bar = 200 µm; b–f: H&E ×400; scale bar = 50 µm).

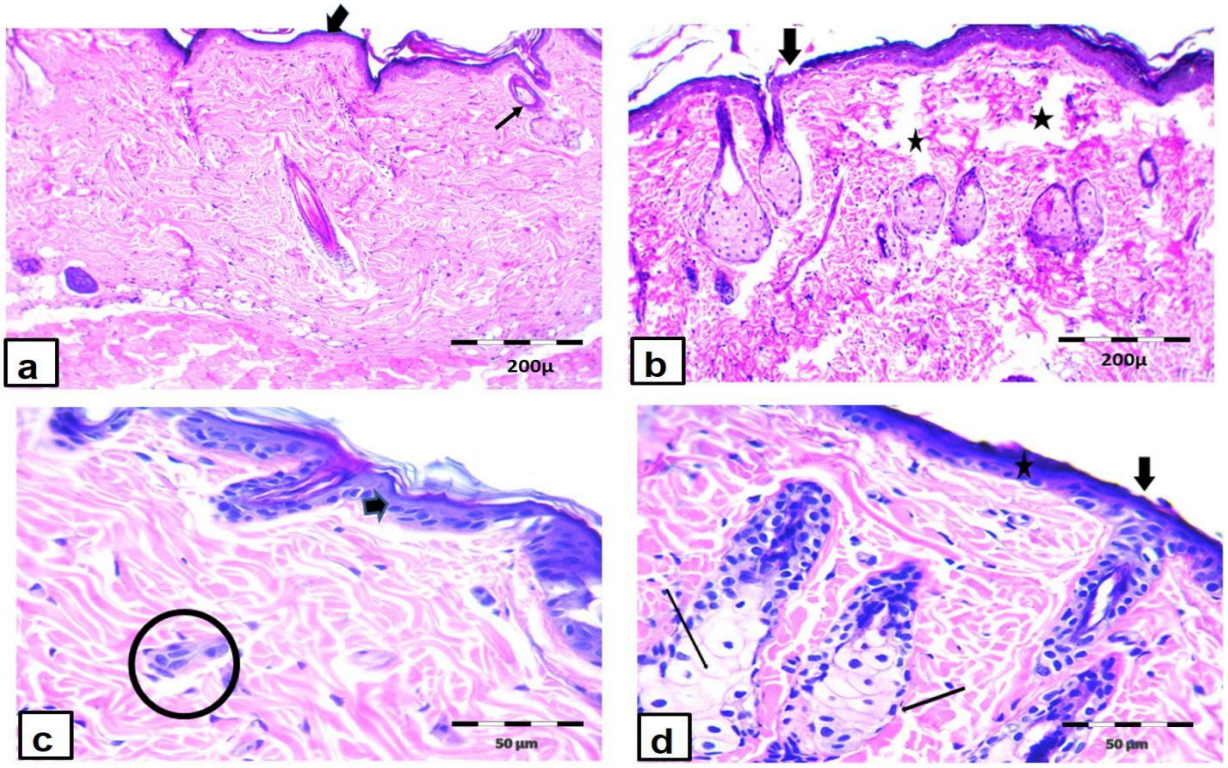

Figure 3. Representative photomicrographs of H&E-stained skin sections of the alopecia-group: (a) Demonstrating a visible thinning of the epidermis (thick arrow) with few hair follicles scattered in the dermis (thin arrow). (b) Showing marked spacing of collagenous fibers in the dermis (★) along with thinning of the epidermis (thick arrow). (c) Showing degenerated hair follicles (circle) associated with reduced epidermal thickness (thick arrow). (d) Showing lobulated sebaceous glands (thin arrows) with partial loss of the stratum corneum (thick arrow) and thinning of the epidermis (★). (a,b: H&E ×100; scale bar = 200 µm;c,d:H&E ×400; scale bar = 50 µm).

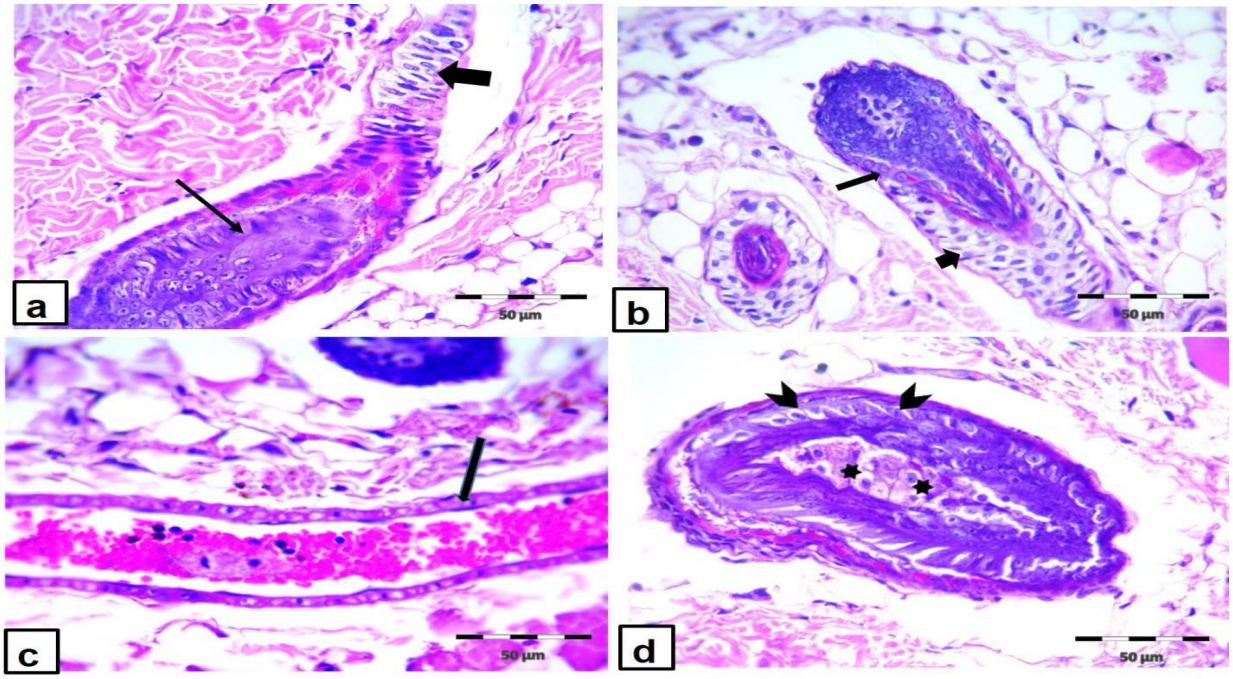

Figure 4. Representative photomicrographs of H&E-stained skin sections in the alopecia-group: **(a)** Showing a catagen hair follicle with epithelial strand (thick arrow) connected to the dermal papilla (thin arrow). **(b)** Showing another catagen hair follicle with the epithelial strand (thick arrow) attached to the dermal papilla (thin arrow). **(c)** Showing a congested blood vessel (black arrow). **(d)** Showing a degenerated anagen hair bulb with vacuolated dermal papilla cells (arrowheads) and vacuolated matrix cells (★). (H&E ×400; scale bar = 50 µm)

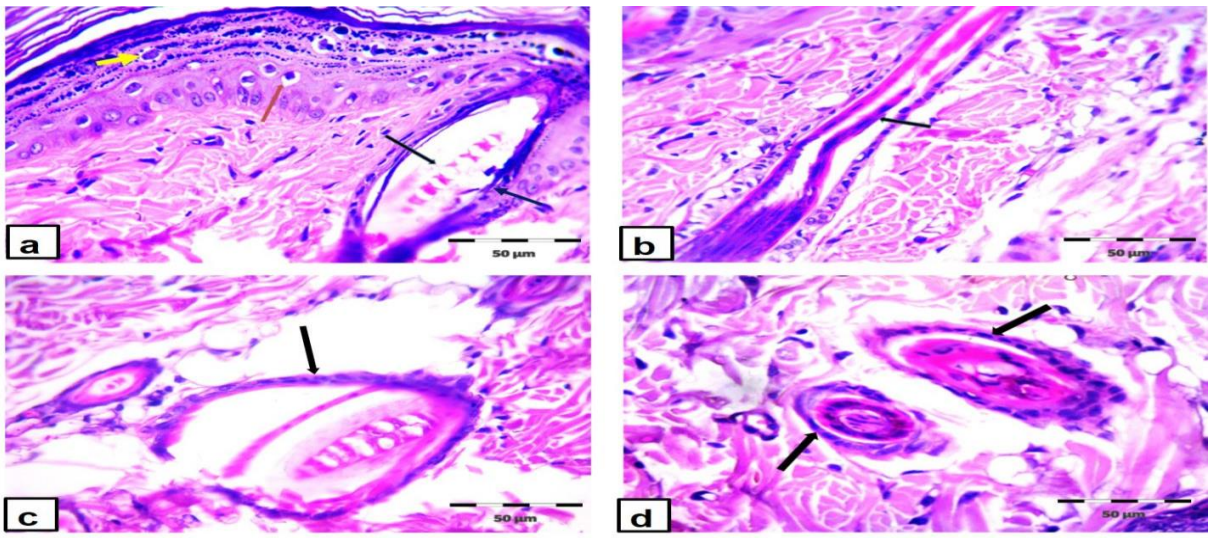

Figure 5. Representative photomicrographs of H&E-stained skin sections of the alopecia-group: (a) Illustrating distorted epidermal cells (yellow arrow), some vacuolated with deeply stained eccentric nuclei (red arrow), together with disruption and degeneration of the hair follicle at the level of the root sheaths (black arrows). (b) Showing disruption and degeneration of hair root layers including medulla, cortex, inner root sheath, and outer root sheath (black arrow). (c) Showing degeneration and separation of hair follicle at the level of the root sheaths (black arrow). (d) Showing transverse sections of hair follicles with degenerative changes and disrupted root layers (black arrows). (H&E ×400; scale bar = 50 µm).

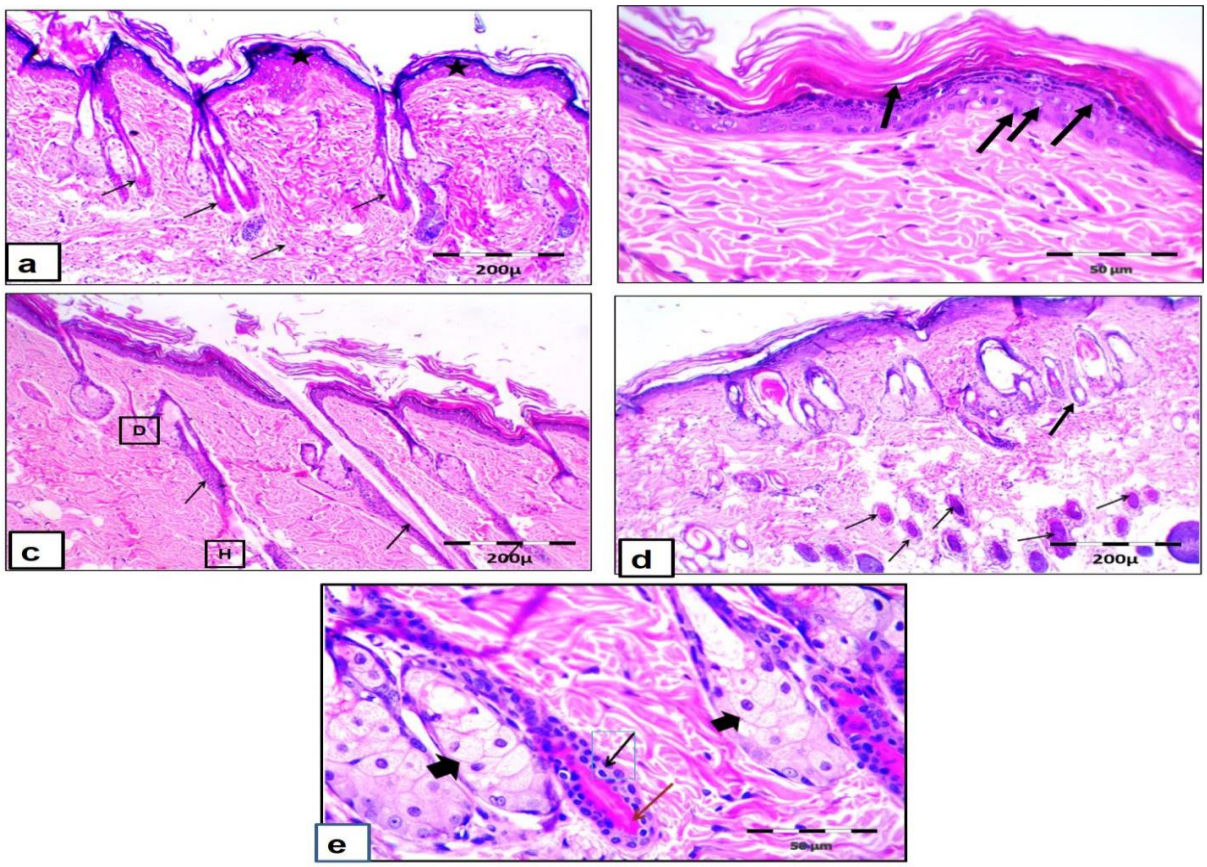

Figure 6. Representative photomicrographs of H&E-stained skin sections of the SVF-treated group: (a) Revealing a noticeable reduction in epidermal thickness (★) with a notable increase in number of hair follicles (arrows). (b) Showing layers of the epidermis: stratum basale (black arrow), stratum spinosum (red arrow), stratum granulosum (yellow arrow), and stratum corneum (green arrow). (c) Showing many hair follicles (arrows) reaching deep layers of the dermis (d) and hypodermis (H). (D) Showing abundant hair follicles distributed within the dermis (arrows). (e) Showing an apparently normal sebaceous gland (thick arrow), with club hair (red arrow) and matrix cells forming a new hair (thin black arrow). (a,c,d: H&E ×100; scale bars = 200 µm; b,e : H&E ×400; scale bars = 50 µm).

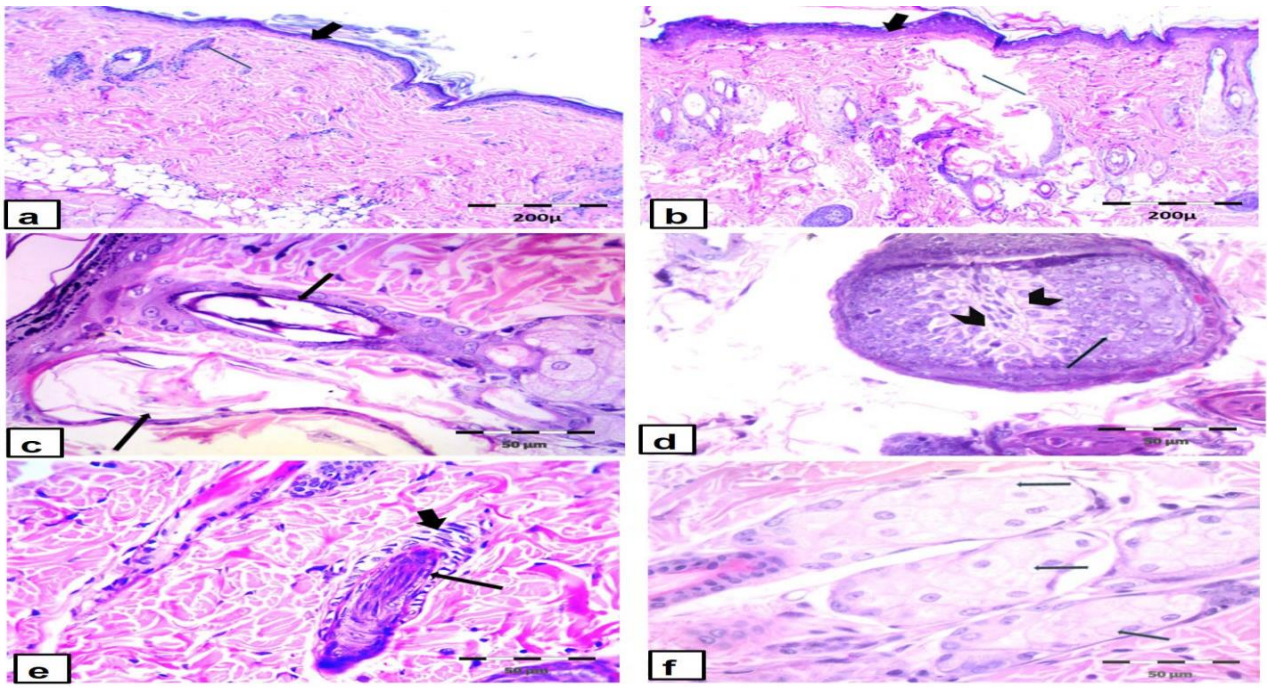

Figure 7. Representative photomicrographs of H&E-stained skin sections of the recovery group: (A) Demonstrating a reduced in thickness of epidermis (thick arrow) and few scattered hair follicles (thin arrow). (B) Showing thinning of the epidermis (thick arrow) associated with widened collagen bundles in the dermis (thin arrow). (C) Showing destructed hair follicles (black arrows). (D) Showing vacuolation and swelling of dermal papilla cells (arrowheads) together with vacuolated matrix cells (black arrow). (E) Showing a catagen follicle characterized by an epithelial strand (thick arrow) attached to the dermal papilla (thin arrow). (F) Illustrating lobulated sebaceous glands (black arrows). (a,b: H&E ×100; scale bars = 200 µm; c-f: H&E ×400; scale bars = 50 µm).

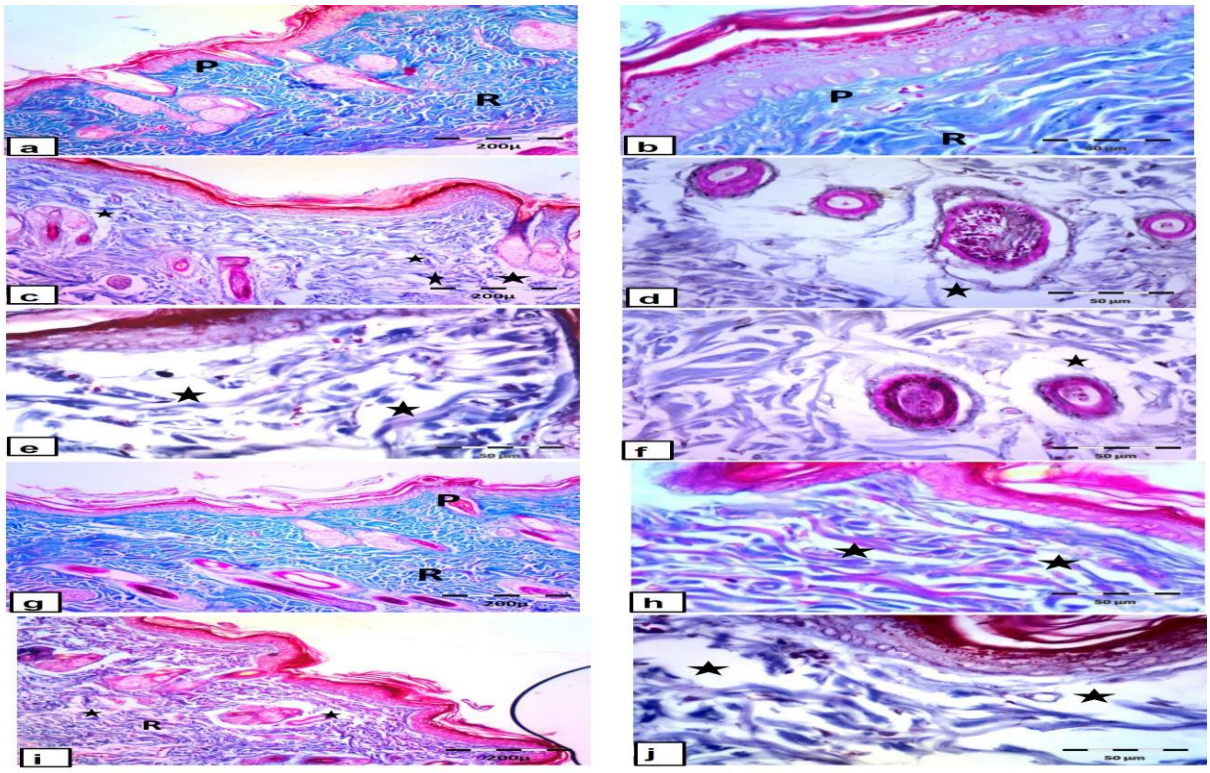

Figure 8: Representative photomicrographs of Mallory's trichrome–stained rat skin sections from the experimental groups. (a, b) Control group: (a)Demonstrating thin, delicate, irregularly arranged collagen fibers in the papillary layer (P). (b) showing coarse, wavy, regularly organized collagen bundles in the reticular layer (R). (c–f) Alopecia- group: (c) showing widening and separation between collagen fibers (★) within the dermal layer. (d) showing disrupted collagen bundles with irregular, loosely arranged fibers and expanded inter-fibrillar spaces (★). (e, f) showing pronounced loosening and disorganization of collagen

fibers (★). (g, h) SVF-treated group: (g) showing apparently normal organization of collagen fibers in both papillary and reticular dermal layers. (h) showing minimal widening between collagen fibers (★) with preservation of the overall dermal architecture. (i, j) Recovery group: (i) showing widening and separation between collagen fibers (★). (j) showing loosening and disorganization of collagen bundles (★). (a, c, e, g, i: Mallory's Trichrome ×100; scale bars = 200 µm; b, d, f, h, j: Mallory's Trichrome ×400; scale bars = 50 µm).

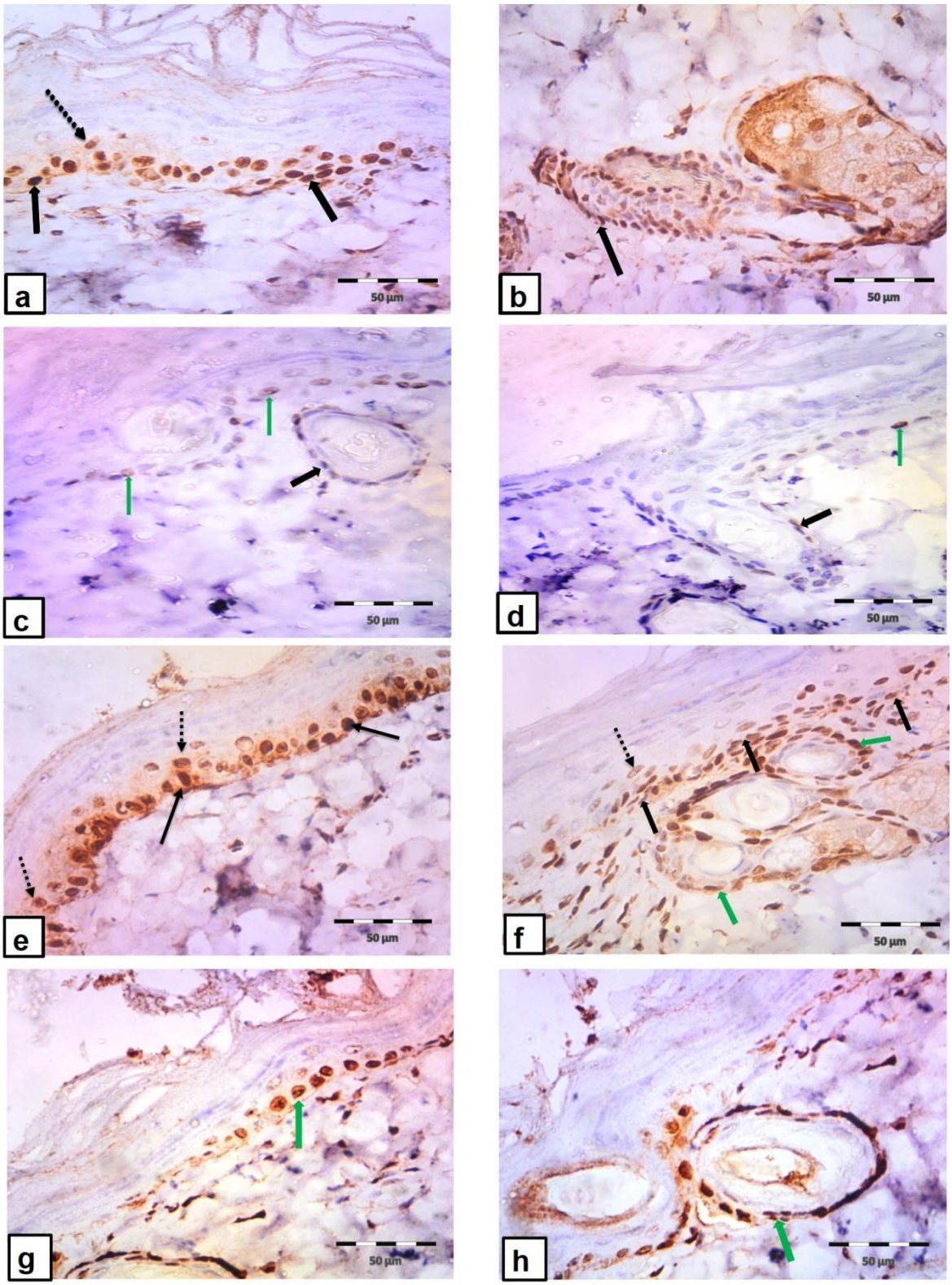

Figure 9: Representative photomicrographs of rat skin sections immuno-stained for Ki67.
(a, b) Control group:(a) showing many cells with positive nuclear expression in the basal cell layer (arrows) and prickle cell layer (dotted arrow). (b) showing many cells with positive nuclear expression within the hair follicles (arrow) (c) Alopecia- group:

showing scattered cells with positive nuclear expression in the stratum basale (green arrows) and within the hair follicles (black arrow). (d, e) SVF-treated group:(d) showing numerous cells with positive nuclear expression in the basal (arrows) and prickle cell layer (dotted arrow). (e) showing numerous cells with positive nuclear expression in the basal (black arrows), prickle (dotted arrow), and within the hair follicles (green arrows). (f, g) Recovery group:(f) showing some cells with positive nuclear expression in the basal cell layer (arrow). (g) showing some cells with positive nuclear expression within the hair follicles (arrow). (Ki67 immunohistochemistry ×400; scale bars = 50 µm).

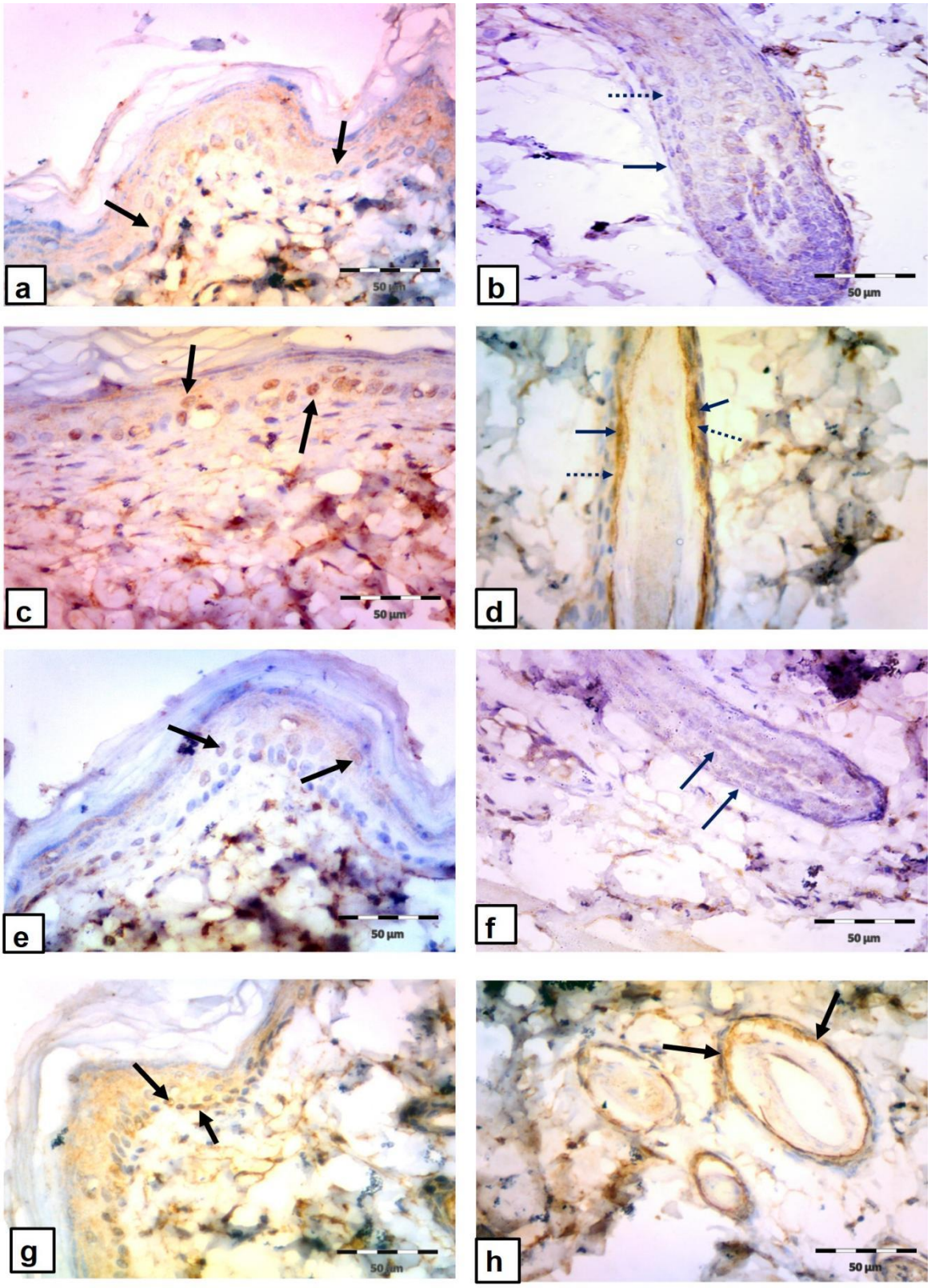

Figure 10: Representative photomicrographs of rat skin sections immuno-stained for activated caspase-3. (a, b) Control group: (a) showing faint positive cytoplasmic expression among cells of the epidermis (arrows). (b) showing negative nuclear and cytoplasmic expression in cells of the inner (dotted arrow) and outer root sheath (arrow) of the hair follicle. (c, d) Alopecia - group: (c) showing many cells with positive nuclear expression in the epidermis (arrows). (d) showing strong positive nuclear (arrows) and cytoplasmic expression (dotted arrows) in cells of the outer root sheath of the hair follicle. (e, f) SVF-treated group: (e) showing faint positive nuclear expression in the cells of the epidermis (arrows). (f) showing negative immune expression in the inner and outer root sheath of the hair follicle (arrows). (g, h) Recovery group: (g) showing many epidermal cells with positive nuclear and cytoplasmic expression (arrows). (h) showing positive expression in the cells of the outer root sheath of the hair follicle (arrows). ((a–h: Activated caspase-3 immunohistochemistry ×400; scale bars = 50 µm).

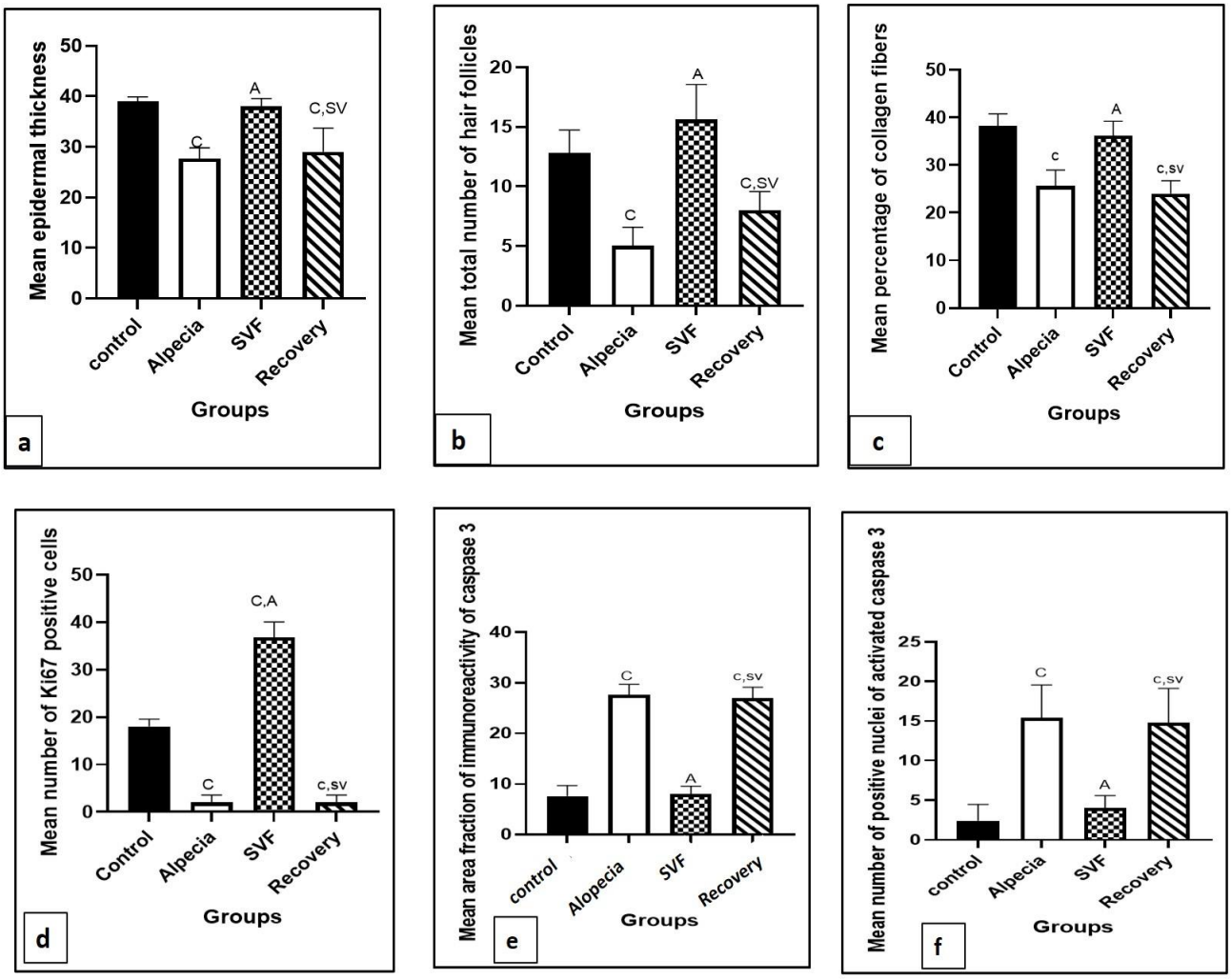

Figure 11. Bar charts illustrating the morphometric parameters in the experimental groups. (a) Mean epidermal thickness. (b)Mean total number of hair follicles. (c) Area percentage of collagen fibers. (d) Mean number of Ki 67 positive cells. (e) Mean area fraction of activated caspase-3 immunoreactivity. (f) Mean number of activated caspase-3 positive cells. Data are expressed as mean ± SD. Significant differences: c versus control group, a versus alopecia group, sv versus SVF-treated group. $p < 0.05$ was considered statistically significant

DISCUSSION

Androgenic alopecia (AGA) is one of the most common causes of hair loss which is characterized by a gradual miniaturization of hair follicles. It is predominantly influenced by androgens in genetically susceptible people [2]. The stromal vascular fraction (SVF), extracted from subcutaneous fat, has lately garnered interest as a regenerative treatment for androgenetic alopecia (AGA) because of its abundant supply of mesenchymal stem cells and endothelial progenitor cells that produce growth factors facilitating tissue repair and regeneration [15].

SVF is proposed to promote hair regrowth by facilitating angiogenesis, regulating inflammation, and activating the Wnt/β-catenin pathway, potentially mitigating the pathological alterations in AGA [1].

This study investigated the histological alterations in rat skin associated with androgenetic alopecia and assessed the efficacy of stromal vascular fraction cells in ameliorating these histological abnormalities. This study also examined the immunoreactivity

of Ki67 as a proliferation marker and activated-caspase-3 as an apoptotic marker. Also evaluated the level of testosterone, Malondialdehyde (MDA), reduced glutathione (GSH)and Wnt family member 3 (WNT3) in the serum, as well as the levels of Dickkopf-related protein 1 (DKK1) in skin tissues among several groups.

The biochemical findings of this study offer essential insights into the mechanisms underlying androgenic alopecia (AGA), presenting compelling evidence for the pathophysiological role of testosterone-induced oxidative stress and disruption of Wnt signaling, while also emphasizing the potential modulatory effects of SVF therapy.

Testosterone levels were markedly higher in the alopecia group than in the control group, corroborating the androgen-dependent characteristic of hair follicle shrinking [16]. The pathogenic mechanism is chiefly facilitated by the local conversion of testosterone to dihydrotestosterone (DHT) via 5α-reductase in dermal papilla cells. Dihydrotestosterone (DHT) has a heightened affinity for androgen receptors, and its binding triggers signaling pathways that reduce the anagen phase, initiate premature entry into catagen, and facilitate progressive follicular shrinking [2].

DHT signaling has been demonstrated to inhibit the Wnt/β-catenin pathway, which is essential for the activation of hair follicle stem cells and the onset of anagen phase. The hormonal disruption continued in the recovery group (Group IV), suggesting a prolonged androgenic impact despite the discontinuation of the inciting drug [17].

Notably, SVF-treated rats (Group III) demonstrated a substantial decrease in testosterone levels, indicating a potential downregulation of androgenic activity and increased local clearance. This impact could be ascribed to the paracrine function of mesenchymal stem cells derived from the stromal vascular fraction, which release anti-inflammatory cytokines and growth factors that regulate androgen receptor signaling, inhibit 5α-reductase activity, and reestablish the equilibrium of Wnt/β-catenin signaling essential for hair follicle cycling [1]. This aligns with the findings of El-Khalawany et al. [7], who studied the Effectiveness of self-derived stromal vascular fraction in treating androgenic alopecia.

The current study demonstrated markedly increased serum MDA levels and reduced GSH in both the alopecia and recovery groups. These changes indicate that androgen exposure induces oxidative stress, potentially leading to hair follicle damage and miniaturization by disrupting redox equilibrium and exacerbating cellular lipid degradation. These findings correspond with Prie et al. [18], who documented elevated plasma MDA and diminished antioxidant capacity in individuals with androgenic alopecia. Comparable results have been noted in other cohorts, revealing increased MDA levels and reduced antioxidant enzyme activity in alopecia patients relative to controls [18, 19]. The SVF therapy resulted in a observed reduce in serum MDA and a considerable rise in GSH levels, indicating that SVF has antioxidative advantages. This action may be facilitated by the release of antioxidant enzymes and growth factors which reinforce the tissue's innate protective mechanisms [9].

Oxidative stress is recognized to induce premature apoptosis and follicular regression by impairing proteins, lipids, and DNA in hair follicle cells (Prie et al., 2016; Cwynar & Olszewska Słonina, 2020). Increased Reactive Oxygen Species (ROS) cause hair loss and cycle termination by endangering keratinocyte and dermal papillae survival [20].

The therapeutic advantages of SVF in androgenic alopecia can be primarily ascribed to its function in restoring oxidative equilibrium within the hair follicle milieu. Our findings in this study align with those of Mantovani et al. [9], who documented the importance of SVF in treating AGA and suggested that SVF functions by diminishing oxidative stress through a reduction in MDA and restoration of GSH. Nonetheless, some studies have reported conflicting results concerning the antioxidant efficacy of SVF treatment. Lee et al. [21] noted that while SVF enhances local tissue oxygenation, its long-term impact on oxidative stress indicators may be affected by the mode of administration and dose. Fukuoka and Suga [22] observed no significant differences in oxidative measures among some alopecia patients treated just with SVF, indicating that combination therapy may be necessary to attain substantial antioxidant advantages.

The canonical Wnt/β-catenin signaling pathway is essential for the maintenance and regeneration of hair follicles. The present study revealed a significant decrease in serum levels of WNT3 in both the alopecia and recovery groups, suggesting blocking of the Wnt/β-catenin signaling pathway.The noted increase of WNT3 after SVF therapy indicates a reactivation of this essential signaling pathway, aiding in follicular healing and regeneration. This conclusion aligns with the studies conducted by Liu et al. [23]and Yan et al. [15].

WNT3 has been demonstrated to facilitate the transition from the telogen to anagen phase and preserve the integrity of dermal papilla cells and hair follicles [2]. Furthermore, exosomes produced from SVF have been shown to promote follicular proliferation and activate WNT3/β-catenin signaling [9].

Conversely, not all studies concur that SVF is an adequate stimulator of Wnt signaling; Pozo-Pérez et al. [24] contended that while MSC-derived products can modulate Wnt pathways, the effect is significantly context-dependent and may be affected by the patient's baseline inflammatory status or hair cycle phase. Furthermore, some studies indicated little or absent elevation in Wnt-related gene expression following SVF treatment in the absence of Wnt agonists [25].

DKK1 is a powerful antagonist of the Wnt/β-catenin pathway and is involved in triggering premature catagen phase and follicular regression in androgenic alopecia [26]. The present analysis revealed that tissue DKK1 levels were markedly increased in both

the alopecia and recovery groups, suggesting ongoing inhibition of Wnt signaling after the termination of androgenic exposure [27]. In contrast, SVF administration markedly reduced DKK1 expression, reinforcing the notion that SVF might mitigate Wnt inhibition and provide a follicle-supportive environment [28].

The current study's findings corroborate the inhibitory impact of SVF on DKK1; however, some authors have argued this mechanism. Chen et al. [29] noted that although there was clinical improvement in alopecia animals treated with SVF, DKK1 expression did not change, indicating that other pathways, such as Bone Morphogenetic Protein (BMP) or Notch, may potentially play a role in the therapeutic response.

The sustained increase of DKK1 in the recovery group corresponds with the established enduring effects of androgen exposure on follicular signaling. The noted reduction in DKK1 following SVF delivery may signify a pivotal mechanism of therapeutic action by alleviating the inhibitory effect on Wnt signaling, hence facilitating normal follicular cycle and regeneration [30].

Histological examination with H&E demonstrated typical histological characteristics of the control group's skin, exhibiting well-defined epidermal layers, a structured dermis consisting of papillary and reticular layers, and many anagen-phase hair follicles. The hair bulb and dermal papilla were intact, and the sebaceous glands were of normal size. These data align with healthy, actively cycling hair follicles and indicate the histological characteristics of the anagen phase [31].

Examination of alopecia group demonstrated characteristic degenerative alterations indicative of the recognized pathophysiology of androgen-induced hair loss. The alterations encompassed a reduction in epidermal thickness and a decreased number of hair follicles [32]. Furthermore, the analysis disclosed degeneration of follicular bulbs and a preponderance of catagen and telogen follicles. The morphological alterations were quantitatively supported by morphometric analysis, revealing a marked reduction in thickness of epidermis and total hair follicle count in comparison to the control group ($P<0.05$). These findings align with those of Kidangazhiathmana and Santhosh [33], who documented the effects of DHT which binds with high affinity to androgen receptors in dermal papilla cells (DPC), modifying gene expression in a way that interferes with the hair growth cycle. It facilitates the early transition of follicles from the anagen phase to the catagen phase, leading to reduced follicular size and eventual hair loss [10]. This androgenic activity hinders the release of growth factors, including Insulin-like Growth Factor 1 (IGF-1) and Vascular Endothelial Growth Factor (VEGF), by dermal papilla cells, therefore impairing the survival and proliferation of matrix keratinocytes [34].

DHT induces oxidative stress by elevating reactive oxygen species (ROS) generation and causing mitochondrial malfunction in dermal papilla cells (DPCs), resulting in apoptosis and structural degradation of the hair bulb [35]. The oxidative damage was histologically apparent in this group, characterized by vacuolation and degeneration of dermal papillae and matrix cells, consistent with the findings of Nada et al. [36]. Additionally, dermal vascular congestion seen in tissue sections may signify impaired microvascular supply, restricting oxygen and nutrient access to the follicle and exacerbating apoptosis-induced damage [37].

The alterations noted in alopecia-group illustrate the intricate interaction of hormonal signaling, oxidative damage, and pathway inhibition that contributes to androgenic alopecia. These modifications emphasize the constraints of spontaneous healing and accentuate the necessity for specific therapies capable of adjusting the molecular and structural disturbances [38].

The SVF-treated group exhibited enhancements in all previously described pathology results. Histological analysis of skin sections from this group demonstrated a marked rise in the hair follicles count, a reduction in telogen hair follicles, and an increased epidermal thickness relative to the alopecia group [12].

The structural enhancements were supported by morphometric analysis, revealing a considerable elevation in both epidermal thickness and total hair follicle count relative to Group II ($P<0.05$). Additionally, this group exhibited reduced vacuolations and swelling of both matrix and dermal papilla cells, signifying a reduction in cellular stress and enhanced follicular integrity. The findings indicate that SVF therapy successfully reinstates follicular structure and function [39].

The regenerative properties of SVF could be ascribed to the local signaling effects of SVF-derived cells, that produce growth factors including Insulin-like Growth Factor 1 (IGF-1), Vascular Endothelial Growth Factor (VEGF), and Hepatocyte Growth Factor (HGF), thereby promoting follicular proliferation, angiogenesis, and dermal remodeling [9, 21].

Our results aligned with the studies conducted by Stevens et al. [40] and Stefanis et al. [41], which examined the stromal vascular fraction and its significance in treatment of AGA. The findings were corroborated by Andia et al. [6], who asserted that SVF cells had the ability for multilineage differentiation owing to the inclusion of mesenchymal stem cells (MSCs) among the SVF cell components. Mesenchymal stem cells (MSCs) have the ability to regenerate damaged tissue by sensing their environment and differentiating in a manner that addresses any necessary repair or replacement of the tissue.

Consistent with these findings, the study by Stachura et al. [42] demonstrated that the manner in which SVF manages AGA involves the promotion of angiogenesis through enhanced tissue hydration, perfusion, and oxygenation, facilitated by the secretion of various growth factors and cytokines, the presence of endothelial progenitor cells, supra-adventitial cells, and the supportive function of MSCs exhibiting pericytic characteristics.

While the current study exhibited notable histological restoration in SVF-treated sections, particularly regarding epidermal thickness and hair follicle architecture, certain reports indicate that SVF may not consistently yield structural regeneration. For example, Kim et al. [12] noted only partial epidermal enhancement in alopecia models post-SVF injection, lacking complete normalization of follicular morphology. Fukuoka and Suga [22] also observed that histological regeneration was modest until the stromal vascular fraction (SVF) was coupled with additional bioactive treatments, such as platelet-rich plasma (PRP) or conditioned media. These data suggest that the regenerating ability of SVF may be affected by parameters such injection method, concentration, or the duration of follicular injury [43].

In the recovery group (Group IV), degenerative alterations persisted, characterized by a thin epidermis and diminished hair follicle count. The observations were verified through quantitative morphometry which indicated a considerable reduction in both epidermal thickness and total hair follicle number relative to the control and SVF-treated groups ($P<0.05$) [4].

Accompanied by consistent evidence of follicular degeneration and enduring manifestations of follicular degeneration, including bulb disruption and vacuolated dermal papillae and matrix cells. The enduring presence of catagen follicles and hypertrophied sebaceous glands indicates that the natural recuperation after androgen cessation is inadequate and fails to reinstate the follicular structure [4]. This further substantiates the efficacy of SVF as a regenerative strategy that may reverse androgen-induced follicular damage and restore skin histoarchitecture [44].

In our research, the histological analysis of skin sections stained with Mallory's trichrome stain yielded significant insights into the condition of dermal collagen fibers, essential indications of extracellular matrix integrity and tissue remodeling [45]. The control group exhibited the characteristic architecture of the dermis: thin, fragile, and loosely organized collagen fibers in the papillary layer, and coarse, wavy, and regularly ordered bundles in the reticular layer. This distribution aligns with the typical histological structure of the skin, wherein type III collagen predominates superficially and changes to thick type I collagen in the deeper dermis, as noted by Kröger et al. [46].

Conversely, the alopecia group had significant widening and separation of collagen fibers, signifying a deterioration of dermal integrity and disrupted collagen homeostasis [47]. The morphometric analysis supported these histological alterations, demonstrating a substantial reduction in the area %of collagen fibers relative to the control group ($P < 0.05$). The findings indicate that pathogenic variables potentially associated with hormonal imbalance or inflammatory mediators may have elevated matrix metalloproteinase (MMP) activity, leading to the breakdown and loosening of collagen fibers, consistent with [45]. The disintegration and spatial disarray of the collagen matrix are characteristic traits in chronic skin injury, aging, or compromised wound healing, indicating a deficiency in the fibroblast-mediated remodeling phase [48].

The histological assessment of the SVF-treated demonstrated a significant decrease in collagen fiber separation and a reconfiguration into a pattern akin to that of the control group [39]. This observation was validated by morphometric data, which indicated a substantial rise in the area % of collagen bundles relative to the alopecia group ($P < 0.05$). These results align with other histological studies that revealed the capacity of SVF to repair and enhance collagen architecture [7, 49]. This indicates a partial repair of the dermal matrix, probably resulting from fibroblast activation and enhanced collagen production, maybe facilitated by the bioactive components in the SVF. Many studies indicate that regenerative therapies, including SVF and PRP, promote collagen deposition and control the function of matrix metalloproteinases (MMPs), enzymes responsible for breaking down the extracellular matrix and remodeling, thus averting excessive collagen depletion and maintaining tissue integrity in AGA [39].

In the recovery group (Group IV), collagen fibers exhibited irregularity, characterized by ongoing widening and separation. Morphometric analysis consistently revealed a significant reduction in the area percentage of collagen fibers compared to both the control and SVF-treated groups ($P < 0.05$). These findings indicate persistent disorganization of dermal connective tissue and suggest that passive recovery alone is inadequate to reverse fibrotic alterations linked to androgen-induced damage. This underscores the essential function of SVF in reestablishing cutaneous homeostasis and averting fibrotic remodeling. These results concurred with the findings of Shi et al. [32].

Ki-67 is a well-established nuclear marker expressed during all active phases of the cell cycle (G1, S, G2, and mitosis), but absent in quiescent (G0) cells, making it a reliable indicator of proliferative activity [50] In the current experment, Ki-67 immunoreactivity was highly expressed in the control group with many positively stained nuclei were seen in the basal and prickle cell layers of the epidermis as well as within the hair follicles. This indicates the elevated proliferative activity of follicles during the anagen period. These findings were verified using morphometric analysis. [36]

Conversely, the alopecia group (Group II) had significantly diminished Ki-67 expression, characterized by just sporadic positively stained nuclei in the basal epidermal layer and within hair follicles. The notable reduction was validated morphometrically, as the quantity of Ki-67–positive cells in the stratum basale, outer and inner root sheaths, and matrix cells was dramatically diminished in comparison to the control group ($P < 0.05$). These findings underscore the inhibitory influence of androgens on follicular proliferation and the induction of premature catagen onset [11]. Recent studies indicate that DHT downregulates Wnt/β-catenin signaling and diminishes growth factor availability, resulting in a reduction in cell cycle progression and stem cell activation within the hair follicle niche [51].

The SVF-treated group demonstrated a significant restoration of Ki-67 expression, with numerous positive nuclei identified in both the basal layer and the prickle layer of the epidermis, as well as abundant positive nuclear expression within hair follicles [9].

Morphometric findings further validated a substantial rise in the quantity of Ki-67–positive cells relative to both the control and alopecia groups ($P < 0.05$). This result demonstrates SVF's capacity to regenerate epidermal and follicular growth. Our observations correspond with previous reports performed by [21, 52].

Concurrently, the recovery group had just a few cells with positive nuclear expression in the basal epidermal layer and within the hair follicles, indicating restricted proliferative recovery. Morphometric analysis revealed a substantial reduction in Ki-67–positive cells relative to the control and SVF-treated groups ($P < 0.05$), suggesting inadequate spontaneous regeneration without therapeutic intervention. This indicates that the restoration of androgen-induced dormancy necessitates the intentional activation of proliferative signaling [53].

Activated caspase-3 is an essential cysteine-aspartic protease that is pivotal in the execution phase of apoptosis. Initially synthesized as an inactive zymogen (procaspase-3), it undergoes activation by proteolytic cleavage by upstream initiator caspases, including caspase-8 or caspase-9, in reaction to intrinsic or extrinsic apoptotic signals. Upon activation, caspase-3 cleaves numerous structural and regulatory proteins within the cell, resulting in chromatin condensation, DNA fragmentation, membrane blebbing, and ultimately, regulated cell death [54]. This physiological function is pathologically exaggerated in conditions like androgenic alopecia (AGA), where dihydrotestosterone (DHT)-induced signaling facilitates premature follicular regression through the upregulation of apoptotic pathways, including increased caspase-3 activation [55].

In the control group, the expression of activated-caspase-3 was very low in epidermal cells with weak or absent in follicular compartments, indicating the low apoptotic activity in healthy, growing follicles [10]. Conversely, the alopecia-group (II) exhibited many epidermal cells with intense nuclear expression, with strong positive nuclear and cytoplasmic expression in the outer root sheath of hair follicles. These were verified through quantative morphometry, which revealed a significant increase in both the mean area fraction of activated caspase-3 immunoreactivity and the number of caspase-3 positive nuclei relative to group1 ($P<0.05$). These results align with studies demonstrating that DHT promotes oxidative stress and initiates death in follicular keratinocytes [10, 35].

The SVF-treated group exhibited a significant reduction in caspase-3 expression, characterized by minimal nuclear positivity in dispersed epidermal cells and a total lack of expression in the inner and outer root sheaths of hair follicles. These findings were corroborated by morphometric analysis, which indicated a substantial decrease in both the mean area fraction of activated caspase-3 immunoreactivity and the count of caspase-3 positive nuclei in comparison to the alopecia group ($P<0.05$) [39]. This indicates a significant anti-apoptotic impact SVF, which serves a protective function in maintaining follicular integrity during androgen-induced stress [56].

SVF mitigates apoptosis by secreting anti-apoptotic factors such as hepatocyte growth factor (HGF), vascular endothelial growth factor (VEGF), and insulin-like growth factor-1 (IGF-1), which enhance cell survival and tissue regeneration. Furthermore, SVF comprises mesenchymal stem cells (MSCs), pericytes, and endothelial progenitor cells that release exosomes capable of downregulating pro-apoptotic genes like Bax (Bcl-2–associated X protein) and upregulating anti-apoptotic mediators such as Bcl-2 (B-cell lymphoma 2) [7, 52].

Conversely, the recovery group showed many epidermal cells demonstrating positive nuclear and cytoplasmic expression, alongside substantial positivity in the outer root sheath of hair follicles. Morphometric analysis corroborated this, revealing a significant elevation in both the mean area fraction of activated caspase-3 immunoreactivity and the number of caspase-3–positive nuclei relative to the control and SVF-treated groups ($P<0.05$). These results imply that spontaneous recovery is inadequate to counteract apoptosis once triggered by androgen exposure, highlighting the efficacy of SVF in reinstating follicular homeostasis [57].

CONCLUSION

This study revealed that androgen-induced alopecia in rat model was accompanied by histopathological and immunohistochemical changes. The administration of adipose-derived stromal vascular fraction (SVF) markedly improved these pathological alterations and exhibited robust regeneration benefits due to its antioxidant, anti-inflammatory, and anti-apoptotic characteristics. These findings underscore the regeneration capacity of SVF therapy in androgenic alopecia and advocate for its evaluation as a viable cell-based therapeutic modality.

REFERENCES

1. Elgobashy A, El-Nefiawy NE, El-Sayed S, Magdy S, Abdelmoez WA. A Review on Androgenic Alopecia: Etiology, Pathogenesis, Pharmacological and Non-Pharmacological Treatment Approaches. Ain Shams Medical Journal. 2024;75(3):587-602. doi: 10.21608/asmj.2024.299393.1282.
2. Shimizu R, Kariya N, Shibata R. Psychological and quality of life impact of androgenetic alopecia in young adults: A cross-sectional study. International Journal of Trichology. 2022;14(2):60–5.

3. Fan H, Huang F. The Pathogenesis and Treatment Progress of Androgenic Alopecia. Journal of Biosciences and Medicines. 2024;12(6):149-58.
4. Asfour L, Cranwell W, Sinclair R. Male androgenetic alopecia. Endotext [Internet]. 2023.
5. Abdin R, Zhang Y, Jimenez JJ. Treatment of Androgenetic Alopecia Using PRP to Target Dysregulated Mechanisms and Pathways. Frontiers in Medicine. 2022;Volume 9 - 2022.
6. Andia I, Maffulli N, Burgos-Alonso N. Stromal vascular fraction technologies and clinical applications. Expert Opinion on Biological Therapy. 2019;19(12):1289-305. doi: 10.1080/14712598.2019.1671970.
7. El-Khalawany M, Shaaban D, Farag A. Efficacy of autologous stromal vascular fraction injection in treatment of androgenetic alopecia: A clinical and trichoscopic evaluation. Journal of Cosmetic Dermatology. 2022;21(2):549–56.
8. Schipper JAM, van Laarhoven CJHCM, Schepers RH, Tuin AJ, Harmsen MC, Spijkervet FKL, et al. Mechanical Fractionation of Adipose Tissue—A Scoping Review of Procedures to Obtain Stromal Vascular Fraction. Bioengineering [Internet]. 2023; 10(10).
9. Mantovani GP, Marra C, De Maria F, Pinto V, De Santis G. Adipose-derived stromal vascular fraction (SVF) for the treatment of androgenic alopecia (AGA): a systematic review. Acta bio-medica : Atenei Parmensis. 2023;94(5):e2023236. Epub 2023/10/18. doi: 10.23750/abm.v94i5.15069. PubMed PMID: 37850761; PubMed Central PMCID: PMC10644943 consultancies, stock ownership, equity interest, patent/licensing arrangement, etc.) that might pose a conflict of interest in connection with the submitted article.
10. Wang W, Wang H, Long Y, Li Z, Li J. Controlling Hair Loss by Regulating Apoptosis in Hair Follicles: A Comprehensive Overview. Biomolecules [Internet]. 2024; 14(1).
11. Elsebay SAG, Nada HF, Sultan NSS, El-Waseef DAE-DA. Comparative histological and immunohistochemical study on the effect of platelet rich plasma/minoxidil, alone or in combination, on hair growth in a rat model of androgenic alopecia. Tissue and Cell. 2022;75:101726. doi: https://doi.org/10.1016/j.tice.2021.101726.
12. Kim SJ, Kim MJ, Lee YJ, Lee JC, Kim JH, Kim DH, et al. Innovative method of alopecia treatment by autologous adipose-derived SVF. Stem Cell Research & Therapy. 2021;12(1):486. doi: 10.1186/s13287-021-02557-6.
13. Suvarna KS, Layton C, Bancroft JD. Bancroft's theory and practice of histological techniques E-Book: Elsevier health sciences; 2018.
14. Basile JR, Castle JT, Redman RS. Immunohistochemical profile of the anti-apoptosis, apoptosis and proliferation markers Bcl-2, caspase-3, p53, and Ki-67 in botryoid odontogenic cysts compared to lateral periodontal cysts and gingival cysts of the adult. Biotechnic & Histochemistry. 2021;96(4):263-8. doi: 10.1080/10520295.2020.1790660.
15. Yan W, Liu J, Xie X, Jin Q, Yang Y, Pan Y, et al. Restoration of follicular β-catenin signaling by mesenchymal stem cells promotes hair growth in mice with androgenetic alopecia. Stem Cell Research & Therapy. 2024;15(1):439. doi: 10.1186/s13287-024-04051-1.
16. Sharara MA, Elfeki EM, Khafagy NH. Assessment of androgenic hormones and other risk factors in Egyptian males with early onset androgenetic alopecia: a case control study. Archives of Dermatological Research. 2025;317(1):552. doi: 10.1007/s00403-025-04041-0.
17. Nascimento B, Miranda EP, Jenkins LC, Benfante N, Schofield EA, Mulhall JP. Testosterone Recovery Profiles After Cessation of Androgen Deprivation Therapy for Prostate Cancer. The Journal of Sexual Medicine. 2019;16(6):872-9. doi: 10.1016/j.jsxm.2019.03.273.
18. Prie BE, Iosif L, Tivig I, Stoian I, Giurcaneanu C. Oxidative stress in androgenetic alopecia. Journal of medicine and life. 2016;9(1):79-83. Epub 2016/12/16. PubMed PMID: 27974920; PubMed Central PMCID: Pmc5152608.
19. Cwynar A, Olszewska-Słonina D, Czajkowski R. The impact of oxidative stress in the androgenic alopecia in women. Advances in Dermatology and Allergology/Postępy Dermatologii i Alergologii. 2020;37(1):119-20. doi: 10.5114/ada.2019.81685.
20. Liang A, Fang Y, Ye L, Meng J, Wang X, Chen J, et al. Signaling pathways in hair aging. Frontiers in Cell and Developmental Biology. 2023;Volume 11 - 2023.
21. Lee CY, Park J, Nam JH. Evaluation of oxidative stress modulation by stromal vascular fraction in skin rejuvenation: limitations and prospects. Antioxidants. 2021;10(4):632.
22. Fukuoka H, Suga H. Hair Regeneration Treatment Using Adipose-Derived Stem Cell Conditioned Medium: Follow-up With Trichograms. Eplasty. 2015;15:e10. Epub 2015/04/04. PubMed PMID: 25834689; PubMed Central PMCID: Pmc4379938.
23. Liu Q, Tang Y, Huang Y, Wang Ja, Yang K, Zhang Y, et al. Insights into male androgenetic alopecia using comparative transcriptome profiling: hypoxia-inducible factor-1 and Wnt/β-catenin signalling pathways*. British Journal of Dermatology. 2022;187(6):936-47. doi: 10.1111/bjd.21783.
24. Pozo-Pérez L, Tornero-Esteban P, López-Bran E. Clinical and preclinical approach in AGA treatment: a review of current and new therapies in the regenerative field. Stem Cell Research & Therapy. 2024;15(1):260. doi: 10.1186/s13287-024-03801-5.
25. Hwang J-H, Lee H-Y, Chung KB, Lee HJ, Kim J, Song K, et al. Non-thermal atmospheric pressure plasma activates Wnt/β-catenin signaling in dermal papilla cells. Scientific Reports. 2021;11(1):16125. doi: 10.1038/s41598-021-95650-y.
26. Tang X, Cao C, Liang Y, Han L, Tu B, Yu M, et al. Adipose-Derived Stem Cell Exosomes Antagonize the Inhibitory Effect of Dihydrotestosterone on Hair Follicle Growth by Activating Wnt/β-Catenin Pathway. Stem Cells International. 2023;2023(1):5548112. doi: https://doi.org/10.1155/2023/5548112.

27. Jung YH, Chae CW, Choi GE, Shin HC, Lim JR, Chang HS, et al. Cyanidin 3-O-arabinoside suppresses DHT-induced dermal papilla cell senescence by modulating p38-dependent ER-mitochondria contacts. Journal of Biomedical Science. 2022;29(1):17. doi: 10.1186/s12929-022-00800-7.
28. Vrapcea A, Pisoschi CG, Ciupeanu-Calugaru ED, Trașcă E-T, Tutunaru CV, Rădulescu P-M, et al. Inflammatory Signatures and Biological Markers in Platelet-Rich Plasma Therapy for Hair Regrowth: A Comprehensive Narrative Analysis. Diagnostics [Internet]. 2025; 15(9).
29. Chen Y, Yu L, Jin X. Stromal vascular fraction partially reverses hair follicle damage but does not normalize DKK1 expression in alopecia models. Stem Cell Research & Therapy. 2019;10(1):54.
30. Mahmoud EA, Elgarhy LH, Hasby EA, Mohammad L. Dickkopf-1 Expression in Androgenetic Alopecia and Alopecia Areata in Male Patients. The American Journal of Dermatopathology. 2019;41(2).
31. Parker GA, Picut CA. Atlas of histology of the juvenile rat: Academic Press; 2016.
32. Shi R, Li S, Liu P, Guo L, Gong S, Wan Y. Effects of testosterone on skin structure and factors related to androgen conversion and binding in Hetian sheep. Tropical Animal Health and Production. 2022;54(4):218. doi: 10.1007/s11250-022-03216-5.
33. Kidangazhiathmana A, Santhosh P. Pathogenesis of Androgenetic Alopecia. Clinical Dermatology Review. 2022;6(2).
34. Jin S-E, Sung J-H. Delivery Strategies of siRNA Therapeutics for Hair Loss Therapy. International Journal of Molecular Sciences [Internet]. 2024; 25(14).
35. Abreu CM, Reis RL, Marques AP. Dermal papilla cells and melanocytes response to physiological oxygen levels depends on their interactions. Cell Proliferation. 2021;54(7):e13013.
36. Nada HF, ElSebay SAG, El-Waseef DAE-DA, Saad NS. A Histological study on the effect of Platelet Rich Plasma on Hair Growth in Male Albino Rat Model of Androgenic Alopecia. QJM: An International Journal of Medicine. 2021;114(Supplement_1):hcab099.10. doi: 10.1093/qjmed/hcab099.010.
37. Deng Z, Chen M, Liu F, Wang Y, Xu S, Sha K, et al. Androgen Receptor–Mediated Paracrine Signaling Induces Regression of Blood Vessels in the Dermal Papilla in Androgenetic Alopecia. Journal of Investigative Dermatology. 2022;142(8):2088-99.e9. doi: https://doi.org/10.1016/j.jid.2022.01.003.
38. Balık AR, Balık ZB, Aktaş A, Neşelioğlu S, Karabulut E, Karabulut AB. Examination of androgenetic alopecia with serum biomarkers. Journal of Cosmetic Dermatology. 2021;20(6):1855-9. doi: https://doi.org/10.1111/jocd.13732.
39. Behrangi E, Rahimi ST, Zare S, Goodarzi A, Ghassemi M, Khodadad F, et al. Evaluation of the effects of adding an adipose tissue-derived stromal vascular fraction to platelet-rich plasma injection in the treatment of androgenetic alopecia: A randomized clinical trial. Skin Research and Technology. 2024;30(4):e13700. doi: https://doi.org/10.1111/srt.13700.
40. Stevens HP, Donners S, de Bruijn J. Introducing Platelet-Rich Stroma: Platelet-Rich Plasma (PRP) and Stromal Vascular Fraction (SVF) Combined for the Treatment of Androgenetic Alopecia. Aesthetic Surgery Journal. 2018;38(8):811-22. doi: 10.1093/asj/sjy029.
41. Stefanis AJ, Groh T, Arenbergerova M, Arenberger P, Bauer PO. Stromal Vascular Fraction and its Role in the Management of Alopecia: A Review. The Journal of clinical and aesthetic dermatology. 2019;12(11):35-44. Epub 2020/02/11. PubMed PMID: 32038756; PubMed Central PMCID: Pmc6937163.
42. Stachura A, Paskal W, Pawlik W, Mazurek MJ, Jaworowski J. The Use of Adipose-Derived Stem Cells (ADSCs) and Stromal Vascular Fraction (SVF) in Skin Scar Treatment—A Systematic Review of Clinical Studies. Journal of Clinical Medicine [Internet]. 2021; 10(16).
43. Butt G, Hussain I, Ahmad FJ, Choudhery MS. Stromal vascular fraction-enriched platelet-rich plasma therapy reverses the effects of androgenetic alopecia. Journal of Cosmetic Dermatology. 2020;19(5):1078-85. doi: https://doi.org/10.1111/jocd.13149.
44. Epstein GK, Epstein JS. Mesenchymal Stem Cells and Stromal Vascular Fraction for Hair Loss: Current Status. Facial Plast Surg Clin North Am. 2018;26(4):503-11. doi: 10.1016/j.fsc.2018.06.010. PubMed PMID: 30213430.
45. Lai IT, Chang Y-H, Chu C-B, Chung P-L, Hsu C-K, Yang C-C. Investigating the role of various extracellular matrix in androgenetic alopecia: Insights from immunostaining and quantitative analysis – A pilot study. Dermatologica Sinica. 2024;42(4).
46. Kröger M, Schleusener J, Jung S, Darvin ME. Characterization of Collagen I Fiber Thickness, Density, and Orientation in the Human Skin In Vivo Using Second-Harmonic Generation Imaging. Photonics [Internet]. 2021; 8(9).
47. Farouk AT, Elgarhy LH, Abdelsalam SF, Mohamed DA, Rabo FA. Androgenetic alopecia updates: pathophysiology diagnosis and treatment. Int J Dermatol Venereology Leprosy Sci. 2023;6(2):108-21.
48. Panchaprateep R, Pisitkun T, Kalpongnukul N. Quantitative proteomic analysis of dermal papilla from male androgenetic alopecia comparing before and after treatment with low-level laser therapy. Lasers in Surgery and Medicine. 2019;51(7):600-8. doi: https://doi.org/10.1002/lsm.23074.
49. Pak J, Lee JH, Pak N, Pak Y, Park KS, Jeon JH, et al. Cartilage Regeneration in Humans with Adipose Tissue-Derived Stem Cells and Adipose Stromal Vascular Fraction Cells: Updated Status. International Journal of Molecular Sciences [Internet]. 2018; 19(7).
50. Uxa S, Castillo-Binder P, Kohler R, Stangner K, Müller GA, Engeland K. Ki-67 gene expression. Cell Death & Differentiation. 2021;28(12):3357-70. doi: 10.1038/s41418-021-00823-x.
51. Chen X, Liu B, Li Y, Han L, Tang X, Deng W, et al. Dihydrotestosterone Regulates Hair Growth Through the Wnt/β-Catenin Pathway in C57BL/6 Mice and In Vitro Organ Culture. Frontiers in Pharmacology. 2020;Volume 10 - 2019.
52. Biniazan F, Stoian A, Haykal S. Adipose-Derived Stem Cells: Angiogenetic Potential and Utility in Tissue Engineering. International Journal of Molecular Sciences [Internet]. 2024; 25(4).

53. Bellani D, Patil R, Prabhughate A, Shahare R, Gold M, Kapoor R, et al. Pathophysiological mechanisms of hair follicle regeneration and potential therapeutic strategies. Stem Cell Research & Therapy. 2025;16(1):302. doi: 10.1186/s13287-025-04420-4.
54. Asadi M, Taghizadeh S, Kaviani E, Vakili O, Taheri-Anganeh M, Tahamtan M, et al. Caspase-3: Structure, function, and biotechnological aspects. Biotechnology and Applied Biochemistry. 2022;69(4):1633-45. doi: https://doi.org/10.1002/bab.2233.
55. Sahoo G, Samal D, Khandayataray P, Murthy MK. A Review on Caspases: Key Regulators of Biological Activities and Apoptosis. Molecular Neurobiology. 2023;60(10):5805-37. doi: 10.1007/s12035-023-03433-5.
56. Srivastava A, Srivastava AK, Pant AB. Strategic Developments for Pre-clinical Safety/Efficacy Studies of Hair Care Products. In: Dwivedi A, Pant AB, Poojan S, Kotak M, Tripathi A, editors. Hair Care Products: Efficacy, Safety and Global Regulation. Singapore: Springer Nature Singapore; 2024. p. 223-73.
57. Martinez-Jacobo L, Ancer-Arellano CI, Ortiz-Lopez R, Salinas-Santander M, Villarreal-Villarreal CD, Ancer-Rodriguez J, et al. Evaluation of the Expression of Genes Associated with Inflammation and Apoptosis in Androgenetic Alopecia by Targeted RNA-Seq. Skin Appendage Disorders. 2017;4(4):268-73. doi: 10.1159/000484530.